Reservoir Quality Assessment of the Upper Permian Chhidru Formation, Salt and Surghar Ranges, Pakistan

Muhammad ZAHIR[1], Muhammad AWAIS[2], Mukhtiar GHANI[3, *], Mohibullah MOHIBULLAH[4], Osman SALAD HERSI[5], Irfan U. JAN[6], Sajjad AHMAD[7] and Hamid IQBAL[8]

[1] *Centre of Excellence in Mineralogy, University of Balochistan, Quetta 87300, Pakistan*
[2] *Department of Geology, University of Swabi, Anbar, Khyber Pakhtunkhwa 23561, Pakistan*
[3] *Geological Survey of Pakistan, HQ, Quetta 87300, Pakistan*
[4] *Department of Geology, University of Balochistan, Quetta 87300, Pakistan*
[5] *University of Regina, Geology 3737 Wascana Parkway Regina, Saskatchewan S4S 0A2, Canada*
[6] *National Centre of Excellence in Geology, University of Peshawar, Peshawar 25000, Pakistan*
[7] *Department of Geology, University of Peshawar, Peshawar 25000, Pakistan*
[8] *Oil and Gas Development Company, Islamabad 44800, Pakistan*

Abstract: The Late Permian succession of the Upper Indus Basin in northeastern Pakistan is represented by the carbonate-dominated Zaluch Group, which consists of the Amb, Wargal and Chhidru formations, which accumulated on the southwestern shelf of the Paleo-Tethys Ocean, north of the hydrocarbon-producing Permian strata of the Arabian Peninsula. The reservoir properties of the mixed clastic-carbonate Chhidru Formation (CFm) are evaluated based on petrography, using scanning electron microscopy (SEM), energy dispersive x-ray spectroscopy (EDX) and x-ray diffraction (XRD) techniques. The diagenetic features are recognized, ranging from marine (isopachous fibrous calcite, micrite), through meteoric (blocky calcite-I, neomorphism and dissolution) to burial (poikilotopic cement, blocky calcite-II-III, fractures, fracture-filling, and stylolites). Major porosity types include fracture and moldic, while inter- and intra-particle porosities also exist. Observed visual porosity ranges from 1.5%–7.14% with an average of 5.15%. The sandstone facies (CMF-4) has the highest average porosity of 10.7%, whereas the siliciclastic grainstone microfacies (CMF-3) shows an average porosity of 5.3%. The siliciclastic mudstone microfacies (CMF-1) and siliciclastic wacke-packestone microfacies (CMF-2) show the lowest porosities of 4.8% and 5.0%, respectively. Diagenetic processes like cementation, neomorphism, stylolitization and compaction have reduced the primary porosities; however, processes of dissolution and fracturing have produced secondary porosity. On average, the CFm in the Nammal Gorge, Salt Range shows promise and at Gula Khel Gorge, Trans-Indus, the lowest porosity.

Key words: sedimentary petrography, diagenesis, hydrocarbon reservoir, Changhsingian, Chhidru Formation, Salt Range, Surghar Range, Pakistan

Citation: Zahir et al., 2021. Reservoir Quality Assessment of the Upper Permian Chhidru Formation, Salt and Surghar Ranges, Pakistan. Acta Geologica Sinica (English Edition), 95(6): 2120–2137. DOI: 10.1111/1755-6724.14764

1 Introduction

The Permian sedimentary strata form a part of the thick Precambrian to Recent sedimentary succession in the Upper Indus Basin, Pakistan (Kummel, 1970). The Permian succession is represented by the Nilawahan and Zaluch groups exposed in the Salt, and Trans-Indus Surghar and Khisor ranges (Kazmi and Abbasi, 2008; Shah, 2009; Fig. 1). The Permian Tethyan carbonate-siliciclastic successions, exposed in the Salt Range and Trans-Indus ranges bear sedimentological and paleontological similarities with time-equivalent successions from Arabia, Turkey and Iran (Stephenson et al., 2013; Ghani, 2017; Ahmad et al., 2018; Jafarian et al., 2018). In addition, the Permian succession represents prolific hydrocarbon-bearing reservoirs in the Middle East, Arabian Peninsula, and the Persian Gulf, which are represented by the Khuff, Akbarah, Unayzah, Dalan and Gharif formations (Stephenson et al., 2013). The hydrocarbon prospects of these regions have been extensively studied (e.g., Egeran and Tasman, 1951; Edgell, 1977; Stephenson et al., 2003; Martin et al., 2008; Stephenson and Al-Mashaikie, 2010; Stephenson et al., 2013). In Pakistan, the Permian succession has been studied for biostratigraphy, paleogeography, and sedimentology (Jan et al., 2009; Shah, 2009; Jan and Stephenson, 2011; Ahmad et al., 2015); however, diagenetic and reservoir studies have not been conducted. The current research focuses on unveiling the reservoir potential of the Pakistani Upper Permian Chhidru Formation (CFm).

This study mainly uses porosity as a key indicator of

* Corresponding author. E-mail: mukhtiar.ghani@gmail.com

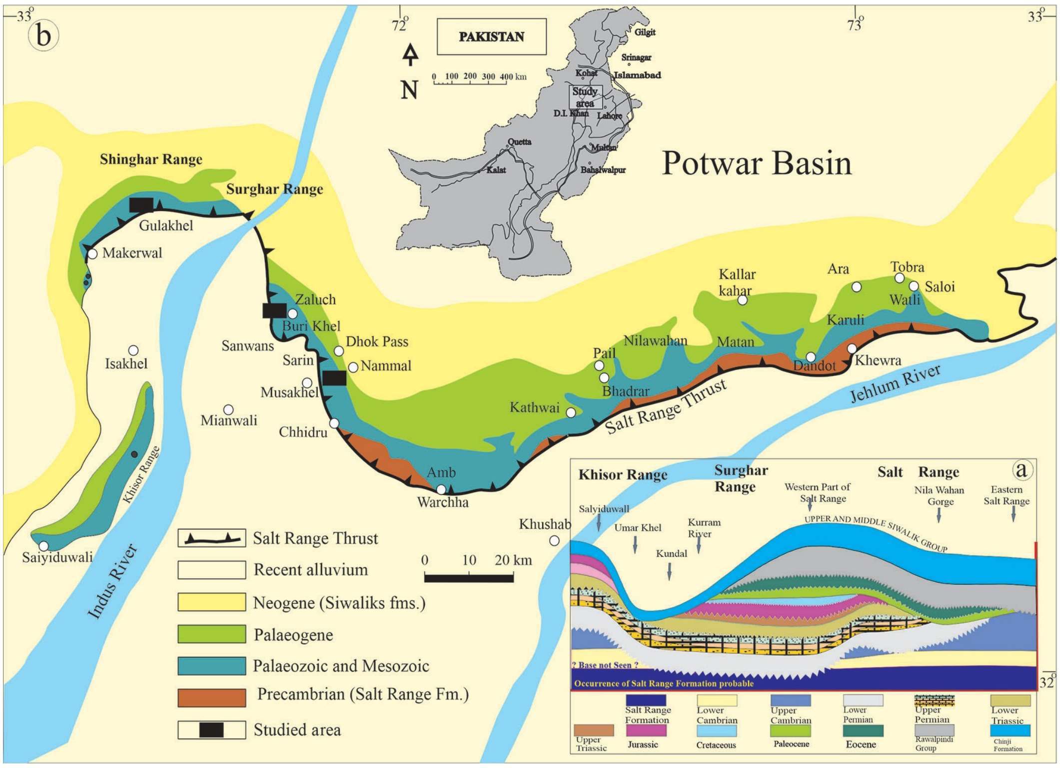

Fig. 1. Regional geological map of the Salt and Surghar ranges, NE Pakistan, showing location of studied sections (after Kazmi and Rana, 1982).

See upper inset figure for the location of study area; and lower inset diagram of stratigraphic succession in the Salt and Trans-Indus, i.e., Surghar, Khisor ranges (after Gee, 1989).

reservoir assessment in terms of its type, origin and amount. Different diagenetic products and their respective processes are recognized and used to propose a diagenetic model for the Changhsingian CFm.

2 Geological Settings

During the Early Permian, the Indian Plate occupied a paleo-position close to the Arabian Plate (Martin et al., 2008; Jan et al., 2009; Stephenson et al., 2013). Rifting during the Late Permian created a space for warm waters, which created a condition suitable for carbonate deposition along the southern edges of Indian and Arabian plates (Angiolini et al., 2003). The late Paleozoic–early Mesozoic rifting resulted in the northwards drift of the Indian plate from the Arabian Plate (Metcalfe, 2006). The Permian succession is thus the last representative of Pangea, which broke up about 250 Ma ago into Laurasia and Gondwana (Torsvik et al., 2010). During the Cretaceous (ca. 130 Ma), the Indian Plate was a separate landmass, which drifted northward and collided with Laurasia during the early Cenozoic, forming different tectonic domains. The northwestern region formed a compressional Himalayan fold-and-thrust regime, while a transgressional Suleiman belt was developed in western Pakistan (Jadoon, 1991). The northwestern region consists of the following four main tectonic zones: (1) the Main Karakoram Thrust (MKT), a suture between Kohistan Island Arc (KIA) and the Eurasian Plate; (2) the Main Mantle Thrust (MMT), a suture between the Kohistan Island Arc and the Indian Plate; (3) the Main Boundary Thrust (MBT), an intraplate thrust where Jurassic successions are thrusted over Miocene, forming the northern border of the Kohat and Potwar fold-and-thrust belts in the Potwar plateau; and (4) the Salt Range Thrust (SRT), a southernmost thrust bringing the Precambrian strata over the Pleistocene deposits of the Punjab Plain (Tahirkheli, 1979; Yeats and Lawrence, 1982). The region is famous for hydrocarbon generation and in production since yearly 20th century (Amir et al., 2017; Ahmad et el., 2019)

The SRT exposed a complete sedimentary succession from Precambrian to Neogene in its hanging wall exposed in the Salt Range area (Fig. 1). The Carboniferous–Permian Gondwanan glaciation, followed by Late Permian rifting and deglaciation, created a favorable setting for deposition of carbonate sediments (López-Gamundí, 2010). In Pakistan, the Late Permian mixed carbonate-siliciclastic setting was established in the northwestern portion of the depositional basin represented by the CFm. This formation shows a thickness variation of 40–80 m throughout the Upper Indus Basin, exposed in the Salt Range and the Trans Indus Basin.

3 Materials and Methods

A total of 47 samples were collected from three different outcrops of the CFm, including 15 samples from the Nammal Gorge, 16 from the Zaluch Nala, western Salt Range and 16 from the Gula Khel Gorge, Surghar Range

(Fig. 1). In the field, outcrop-scale sedimentological features such as bedforms, texture, formational and facies contacts and lithological variations were recorded. Thin section preparation, Scanning Electron Microscopy (SEM), Energy Dispersive X-ray Spectroscopy (EDX) and X-Ray Diffraction (XRD) analysis were conducted at the National Centre of Excellence in Geology, University of Peshawar, Pakistan.

Thin sections were studied for petrographic features, and to understand the detailed diagenetic evolution and reservoir quality assessment. The petrographic studies were conducted at the Centre of Excellence in Mineralogy, University of Balochistan, Quetta. For model composition, point counting, a semi-automatic classification method based on JMicroVision software was employed to estimate the porosity. The samples are housed in archives of Centre of Mineralogy (CEM), University of Balochistan, Quetta, Pakistan.

4 Results and Discussion

4.1 Petrography of the Chhidru Formation

The CFm is divided into four microfacies (Ghani, 2017; Fig. 2) based on Folk's (1959) classification. These microfacies include: (i) siliciclastic mudstone microfacies (CMF-1), (ii) siliciclastic bioclastic wackestone to packestone microfacies (CMF-2), (iii) siliciclastic bioclastic grainstone microfacies (CMF-3), and (iv) graywacke (calcareous) sandstone facies (CMF-4).

The CMF-1 is dominated by a micrite matrix with subordinate silt to fine sand framework with grains of quartz, feldspar, mica and some fossils; this facies is represented by 14 samples: CN-1, 2, 4, 5, 8, 12, CG-1, 4, 8, 9, 13, and CZ-1, 4, 10. The CMF-2 is represented by 14 samples: CN-3, 7, 9, CG-2, 3, 5, 6, 12 and CZ-2, 3, 5, 6, 9, 11. CMF-3 is represented by 8 samples: CN-10, 11, 14, CG-14, 15, and CZ-8, 13, 15. The CMF-4 is dominated by quartz, and some feldspar and mica, with rare fossil content (Ghani, 2017). This facies is represented by 11 samples CN-6, 13, 15, 16, CG-7, 10, 11, and CZ-7, 12, 14, 16, (Fig. 2).

Overall, the framework grains of the CFm are dominated by quartz and bioclasts, such as echinoderm, bryozoan, green algae, fusulinid, brachiopod, gastropod, pelecypod and other unidentified fossils. Rare feldspars and micas are also present in thin section (Fig. 2) and in the respective XRD data (Figs. 3, 4). The matrix is almost exclusively micrite whereas various types of pore-filling cements, both ferroan and non-ferroan calcite, are present. Monocrystalline quartz, very few feldspar grains and fossil fragments dominate the sandy grainstone and sandstone microfacies and quartz-wacke to sandstone facies. The quartz grains are angular to sub-rounded and well sorted (Fig. 2). Diagenetic features, such as micritization, fracture-filled calcite cement, neomorphism, dissolution, compaction and microstylolites have been observed (Figs. 10, 11). There are floating pointed grains in the matrix of all microfacies, but in CMF-4 microfacies, grains are more prominent. In all facies, the quartz grains show a variation from fine- to coarse-grained and feldspar is fine- to medium-grained.

Overall, the petrography shows that the CFm is grains-dominant with a majority of calcite, quartz and biota; the matrix is mainly micritic with some cement, with a few feldspars, muscovite, and pore spaces. The allochems contain poorly to well-preserved fossils of various invertebrates and some unidentified bioclasts (Fig. 2). The micritic matrix also contains sparry calcite and ferroan calcite cement.

4.2 Clay mineralogy using XRD and EDX analyses

4.2.1 XRD results

The XRD results of 11 samples from different facies (Figs. 3–5) represent a multi-mineral system. XRD provided information on the rock mineral(s) composition and clay typing. The system represents a mixed carbonate-siliciclastic setting. Data show presence of calcite, quartz, feldspar, dolomite, ankerite, siderite, montmorillonite and kaolinite in different samples of the studied outcrop sections. The Gula Khel Section samples, i.e., CG-2 (Fig. 4e), CG-5 (Fig. 4f) and CG-7 (Fig. 3d), consist of calcite, quartz, feldspar, dolomite, siderite, ankerite, illite and kaolinite (Fig. 5). Similarly, the Zaluch Nala Section samples, i.e., CZ-2 (Fig. 4c), CZ-7 (Fig. 3c), CZ-12 (Fig. 3e) and CZ-15 (Fig. 4d), consist of calcite, quartz, feldspar, siderite, illite and kaolinite (Fig. 5). Likewise, the Nammal Gorge Section samples, i.e., CN-2 (Fig. 3b), CN-4 (Fig. 3a), CN-09 (Fig. 3b) and CN-11 (Fig. 4a), consist of calcite, quartz, feldspar, ankerite, siderite, illite and kaolinite (Fig. 5). All samples studied are dominated by carbonate (calcite) content except for sample CZ-7 of the Zaluch Nala Section, which is dominated by clastic sediments, predominantly quartz with subordinate feldspar. The ankerite and dolomite are present in very few samples and their percentages are also quite low. Siderite is present in several samples with relatively higher percentages. Illite is present in all samples with quite low percentages. Kaolinite is also present in several samples.

Calcite, quartz and feldspar are the framework grains of the mixed carbonate-siliciclastic sediments/rock. Calcite, dolomite, ankerite and siderite are most probably different types of carbonate cements. Calcite and dolomite mostly form as pore-filling cements while siderite is mostly found as scattered crystals, nodules and spherules in the rock (Morad, 1998). In addition, ankerite also occurs in fractures and the vugg pore-filling phase (Győri et al., 2020).

Dolomite is usually formed in a mixed marine-meteoric environment (Badiozamani, 1973; Awais et al., 2020). Similarly, siderite is reported to form from reducing, sulphate-free pore waters of a marine and mixed marine-meteoric nature (Moore et al., 1992; Morad, 1998). Ankerite is reported to develop in association with clay mineral transformation and/or formed by replacement of dolomite (Hendry et al., 2000; Schmid, 2004). During burial (medium to deep), the cations of iron and manganese are liberated during diagenesis of clay-minerals (i.e., smectite to illite transformation) in siliciclastic rocks and accommodated as replacement and cement phases of dolomite and ankerite (Győri et al., 2020). Clay minerals montmorillonite and kaolinite can be mechanically infiltrated or diagenetically formed (Morad

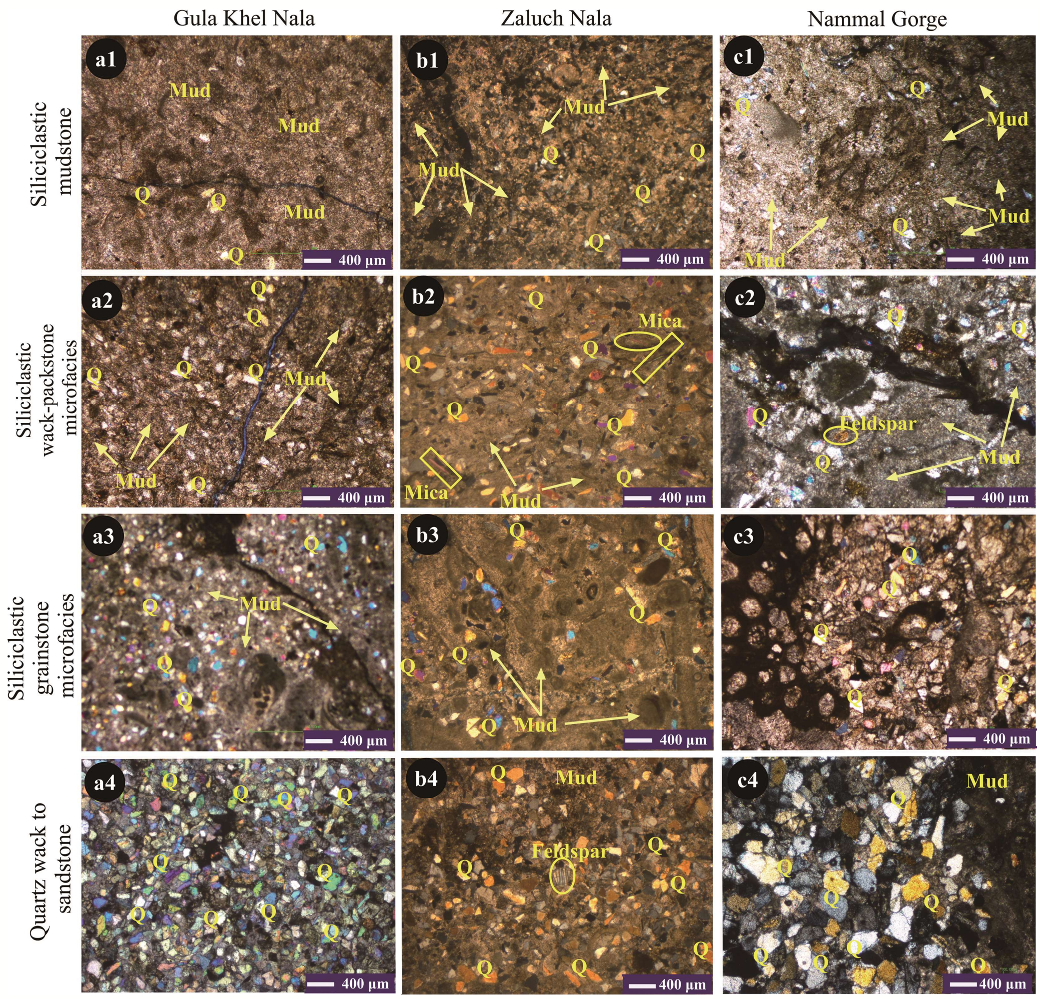

Fig. 2. Photomicrographs represent microfacies of the Chhidru Formation (based on Ghani, 2017).
1–Siliciclastic mudstone microfacies (CMF-1); 2–siliciclastic wacke-packstone microfacies (CMF-2); 3–siliciclastic grainstone microfacies (CMF-3); 4–quartz-wacke sandstone microfacies (CMF-4). Locations: a–Gulakhel Nala; b–Zaluch Nala; c–Nammal Gorge; Q–quartz.

et al., 2000). Kaolinite may be formed by alteration (i.e., dissolution and replacement) of feldspar or diagenetically formed (Ma et al., 2018).

4.2.2 SEM-EDX results

The SEM-EDX analysis of some spots of different samples from the CFm demonstrated the presence of different clay minerals, such as chlorite, illite, kaolinite and feldspar, in association with quartz and calcite (Figs. 6–9).

Chlorite, illite and kaolinite are present (Fig. 6d-001) with quartz and a minor amount of calcite (Fig. 6d-002, 7e-001). Illite, kaolinite, montmorillonite and calcite were found (Fig. 7e-002). Fig. 8e (i.e. 001) shows presence of quartz, calcite (minor quantity) and montmorillonite and Fig. 8e (i.e. 002) shows presence of illite, quartz and calcite (in minor quantity). Fig. 9e (i.e. 001) shows presence of quartz and calcite in minor quantities. Fig. 9 (i.e. 002) indicates calcite only.

Chlorite is documented by the presence of peaks of silicon (Si), aluminum (Al), magnesium (Mg) and iron (Fe) (Fig. 6d). The illite spectrum reflects presence of Si, potassium (K) and aluminum (Al) peaks (Figs. 6d, 8e). In Fig. 6d and 7e (i.e., 002), the peaks of Al and Si are quite close and hence there is a probability for the presence of kaolinite (Welton, 2003). Montmorillonite is confirmed by peaks of Si, Na, Ca and Al (Figs. 7e-002, 8e-001). The EDX spectrum of quartz is reflected by peaks of Si and O (Figs. 6d-002, 7e, 8e, 9e-001). The EDX spectrum of calcite is reflected by the presence of peaks of Ca, C and O (Figs. 6d-002, 7e, 8e, 9e). Chlorine (Cl) in a couple of EDX spectrums might show contamination from nearby grains (Figs. 6d, 8e). Sodium (Na) (Fig. 6d-002) might show contamination from feldspar. There is also presence of trace quantities of Fe, manganese (Mn) and titanium (Ti) in one of the EDX spectra, which is dominated by illite (Fig. 8e-002). There is some phosphorus (P) (Fig. 9c-02), but the absence of phosphorus-based minerals in the EDX and other data, shows that possibly this might have come from apatite as contamination.

These clay minerals are mostly formed by alteration of micas and feldspars (Khan et al., 2018; Worden et al., 2018). In sandstones, the commonly occurring authigenic clay minerals include chlorite, illite, kaolinite, mixed layer illite–smectite and smectite (Khan et al., 2018; Ma et al., 2018; Shehzad, 2019). Likewise, authigenic clay minerals

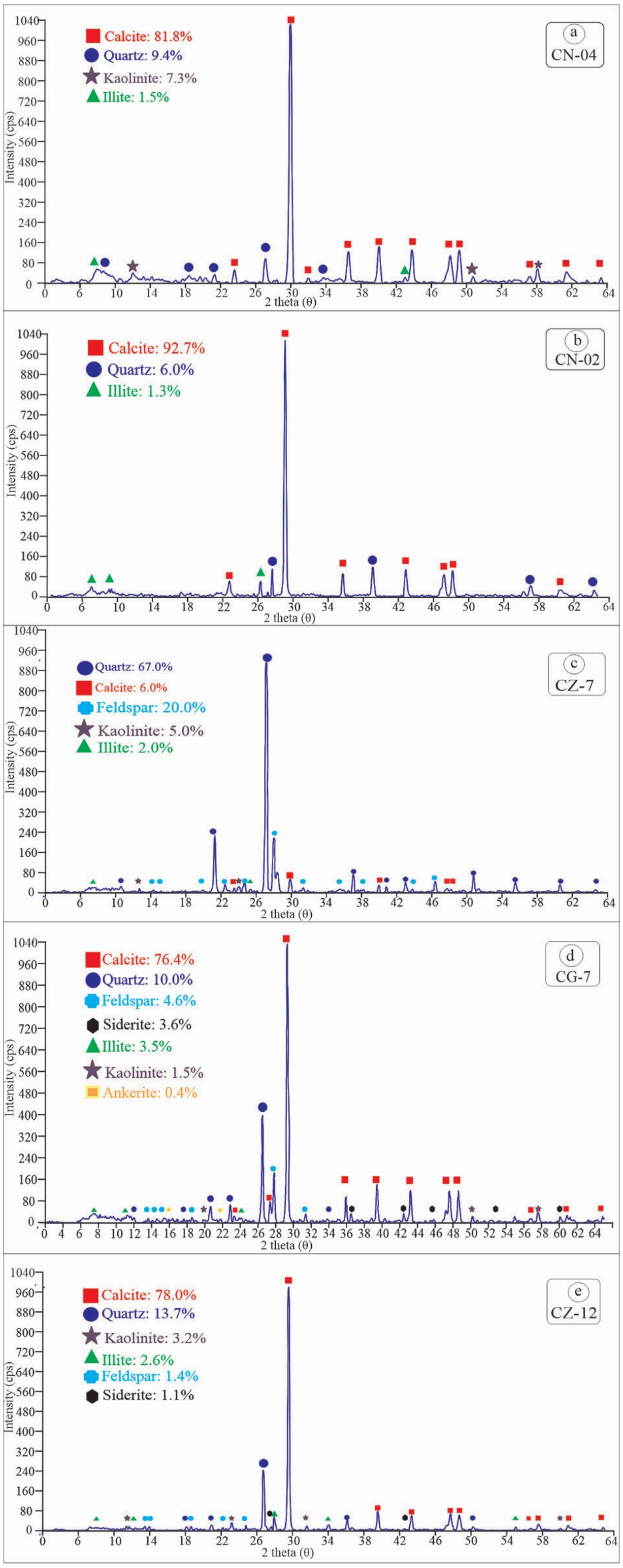

Fig. 3. XRD results of samples from the Chhidru Formation.
The system represents a mixed carbonate-siliciclastic setting: (a) CN-04 is 83.2% calcite, 16.8% quartz with some kaolinite and illite; (b) CN-02 shows 92.4% calcite, 7.6% quartz and ~1.3% illite; (c) CZ-07 is a clastic-dominant facies with 94.9% quartz, 20% feldspar, 5.1% calcite with 5% kaolinite and 2% illite; (d) CG-07 shows 92.4% calcite, 7.6% quartz, with feldspar, illite, kaolinite and ankerite present as traces; (e) CZ-12 has 87.8% calcite, 7.6% quartz with some kaolinite, illite, feldspar and siderite.

encountered in mixed siliciclastic carbonates includes kaolinite and illite (Lü et al., 2017). Montmorillonite is a precursor for different clay minerals such as chlorite and illite (Dunoyer De Segonzac, 1970; Sánchez and Galán, 1995). Lack of montmorillonite reflects considerable burial experienced by some rocks (Dunoyer De Segonzac, 1970). Illite can also be formed by transformation of kaolinite (Zhang et al., 2007).

4.2.3 Clay typing and its impact on reservoir

Clay minerals can occupy different areas in a reservoir, for example, detrital, matrix in intergranular pores, pore filling by authigenic clay minerals, grain coatings, pore-lining rims, and as cements (Zamanzadeh et al., 2011; Baiyegunhi et al., 2017; Khan et al., 2018; Ma et al., 2018; Duan et al., 2020). The presence of clay minerals in different forms in sandstones negatively influences reservoir quality (Khan et al., 2018; Shehzad, 2019). Such minerals occupy pore spaces up to a significant level, thereby reducing the porosity (Shehzad, 2019).

In the CFm, almost all of the identified clay minerals are reported from micropores, thereby demonstrating their occurrence as pore-fillings and hence reducing the porosity of the CFm. Sometimes, clay mineral anthogenesis (chlorite coatings) can preserve primary porosity (Bjørlykke and Jahren, 2012), but this feature is missing in the studied CFm. There are certain possibilities for the occurrence of clay minerals in the micropores of the CFm samples. They might have been mechanically infiltrated or formed during diagenesis, i.e., clay mineral anthogenesis. The clay mineral presence has not only affected the porosity negatively but has also been predicted to have a negative impact on the permeability of the CFm mixed siliciclastic carbonates. Contrarily, the clay minerals might lead to pore development, for example, when clay minerals form by alteration of feldspar and hence porosity is generated during this process (Baiyegunhi et al., 2017; Yuan et al., 2019).

According to Baiyegunhi et al. (2017) and Ma et al. (2018), clay minerals (i.e., chlorite, illite, kaolinite, mixed-layer illite/smectite and smectite) are found as pore-lining rims, pore-filling materials and partially grain-coating in the Permian Ecca Group sandstones of South Africa and Permian Shiqianfeng sandstones of the Bohai Bay Basin of China, respectively. Clay minerals reported as cements and/or pore-filling and pore-linings and reducing the reservoir quality have also been noticed in the Permian Faraghan Formation of Iran and Ridge Sandstone of India (Zamanzadeh et al., 2011; Khan et al., 2018).

4.3 Diagenetic fabric

The CFm has undergone different diagenetic processes of micritization, various stages of cementation, calcite vein filling, neomorphism, dissolution and compaction fractures, e.g., stylolite. These diagenetic features are commonly controlled by grain composition, its texture and presence or absence of micritic mud matrix.

4.3.1 Micritization

One of the key signatures of a marine diagenetic environment is micritization (Khalifa, 2005; El Ghar et al.,

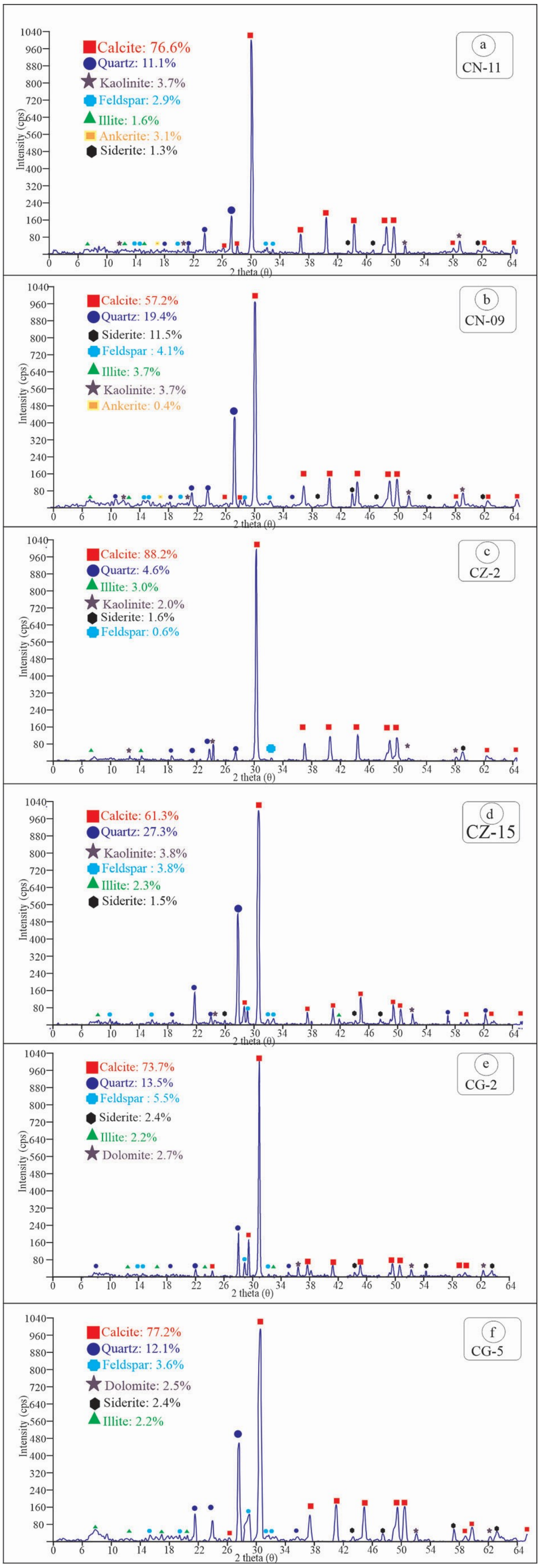

Fig. 4. XRD results of samples from the Chhidru Formation.
All sections possess a multi-mineral system consisting of calcite, quartz, feldspar, kaolinite, siderite, ankerite, illite, and some dolomite. (a) CN-11 mostly consists of 95.3% calcite and 4.7% quartz; (b) CN-09 consists of 75.1% calcite and 24.9% quartz; (c) CZ-02 has 95.2% calcite and 4.8% quartz; (d) CZ-15 is 73.7% calcite and 26.4% quartz; (e) CG-02 has 83.4% calcite and 16.6% quartz; (f) CG-05 consists of 85.7% calcite and 14.3% quartz.

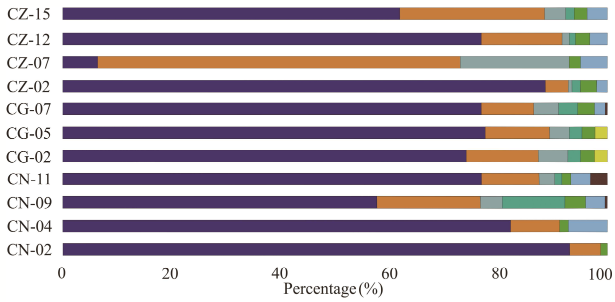

	CN-02	CN-04	CN-09	CN-11	CG-02	CG-05	CG-07	CZ-02	CZ-07	CZ-12	CZ-15
Calcite	92.7	81.8	57.2	76.3	73.7	77.2	76.4	88.2	6	78	61.3
Quartz	6	9.4	19.4	11.1	13.5	12.1	10	4.6	67	13.7	27.3
Feldspar	0	0	4.1	2.9	5.5	3.6	4.6	0.6	20	1.4	3.8
Siderite	0	0	11.5	1.3	2.4	2.4	3.6	1.6	0	1.1	1.5
Illite	1.3	1.5	3.7	1.6	2.2	2.2	3.5	3	2	2.6	2.3
Dolomite	0	0	0	0	2.7	2.5	0	0	0	0	0
Kaolinite	0	7.3	3.7	3.7	0	0	1.5	2	5	3.2	3.8
Ankerite	0	0	0.4	3.1	0	0	0.4	0	0	0	0

Fig. 5. Relative mineralogical abundance from XRD results of all three sections.
The graph shows that the studied samples are carbonate-dominated with rare clastic rich samples. The table shows quantities of the different minerals.

2015). Optically, micrite is a uniform mass of translucent to opaque and very fine-grained calcite, which is mostly formed by degradation of skeletal and non-skeletal grains at the sediment–water interface by endolithic algae, fungi and bacteria (Adams and MacKenzie, 1998; Tucker and Wright, 2009). The preliminary diagenetic phenomena preserved in all samples have texturally modified the CFm. This process of micritization is either selective, i.e., micritization of bioclasts and formation of micrite envelopes or intense, i.e., destroying complete grains (Figs. 10a–g). Such selective micritization is observed in all four microfacies of CFm but is more prominent in the limestone microfacies of the siliciclastic mudstone microfacies (i.e., CMF-1), the siliciclastic wacke–packestone microfacies (CMF-2), and the siliciclastic grainstone microfacies (CMF-3) (Figs. 2, 10). It has affected skeletal grains, preserved in the form of micrite envelopes (Figs. 10f, g), and, at certain intervals, obliterated the internal structure of skeletal grains (Fig. 10c), while in some grains micritic mud has been deposited as internal depositional material (Figs. 10a, b, c, f, g). The intensity of selective micritization varies from partial, on the skeletal grain, such as the micrite envelope, to severe, i.e., completely obliterating the initial fabric (Figs. 10d, e). Petrographically, intact cores of the skeletal and partial-to-severe distorted cores of the skeletal structure are enclosed by micritic envelopes.

Intensive micritization can be cardinal to a completely structureless skeletal body so that the original morphology

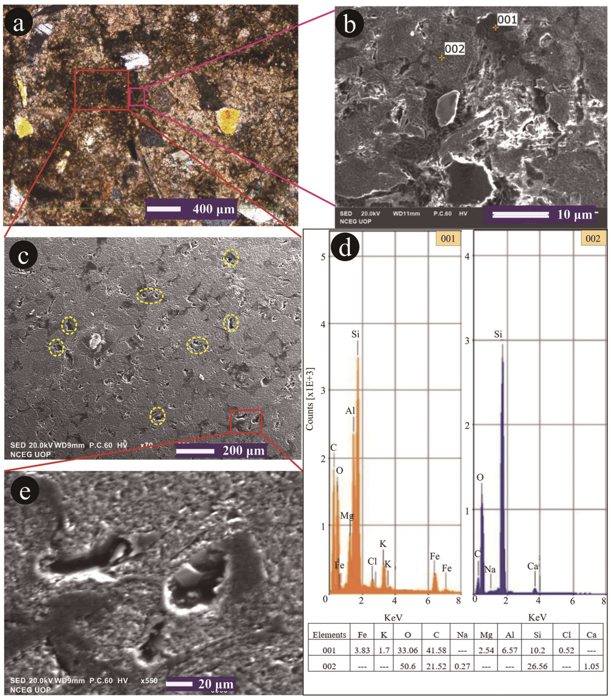

Elements	Fe	K	O	C	Na	Mg	Al	Si	Cl	Ca
001	3.83	1.7	33.06	41.58	---	2.54	6.57	10.2	0.52	---
002	---	---	50.6	21.52	0.27	---	---	26.56	---	1.05

Fig. 6. Photomicrographs, SEM and EDX-based microporosity and elemental composition of selected points of the Chhidru Formation samples.
(a) Photomicrograph of interested zone; (b–c) SEM photomicrographs showing microporosities; (d) graph 001, 002 and table represents the elemental composition of the selected points in photomicrograph b. The number of CEM, University of Balochistan collection are given as below (a) MZK-2009-C1A; (b) MZK-2009-C1B; (c) MZK-2009-C1C; (d) MZK-2009-C1D; (e) MZK-2009-C1E.

of the skeletal grain is difficult to establish (Tucker and Wright, 2009). Some CFm samples show structureless micritic bodies, i.e., micritization has completely obliterated the initial particle (Figs. 10a, d, e).

4.3.2 Neomorphism

Neomorphism represents the procedure of replacement and recrystallization of original carbonate constituents. Since carbonate sediments are a mixture of calcite and aragonite minerals, the term recrystallization cannot be used because mineralogical change may occur in carbonate sediment recrystallization. The process of neomorphism occurs in the presence of water, normally in fine-grained carbonate rocks (Tucker and Wright, 2009). The calcitization of aragonite, dolomite and evaporite minerals are common neomorphic processes in carbonate rocks (Tucker and Wright, 2009).

Aggrading neomorphism, i.e., recrystallization into larger grain size, is observed in the CFm siliciclastic mudstone, siliciclastic wackestone and silicicclastic grainstone microfacies. The conversion of micritic matrix to microspar and sparite is the result of aggrading neomorphism (Figs. 10a, b, i) and with advanced neomorphism, blocky cement was formed (Fig. 10g). The aggrading neomorphism represents marine to burial diagenesis; it affects all three types of the carbonate lithofacies, i.e., mudstone, wackestone to packstone and

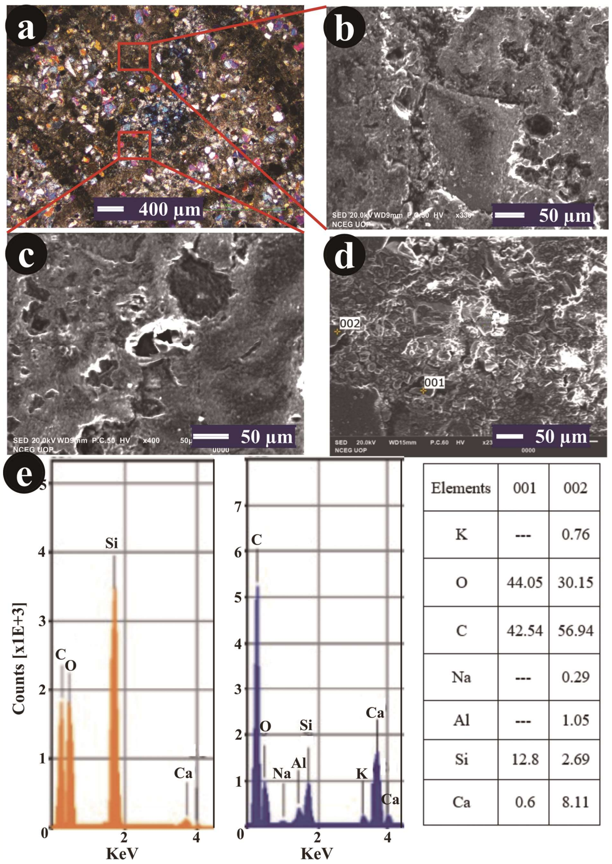

Elements	001	002
K	---	0.76
O	44.05	30.15
C	42.54	56.94
Na	---	0.29
Al	---	1.05
Si	12.8	2.69
Ca	0.6	8.11

Fig. 7. Photomicrograph from the petrographic microscope, SEM and EDX based micro-porosity and elemental composition of the selected points.
(a) Photomicrograph obtained from petrographic microscope of the interested zone; (b–d) SEM photomicrographs showing micro porosities; (e) graph 001, 002 and table represents the elemental composition of the selected points in photomicrograph d. The number of CEM, University of Balochistan collection are given as below (a) MZK-2009-C2A; (b) MZK-2009-C2B; (c) MZK-2009-C2C; (d) MZK-2009-C2D; (e) MZK-2009-C2E.

grainstone (Figs. 10a, b, g, i). The micritic matrix experienced well-established larger blocky calcite, followed by a decrease towards the boundaries (Fig. 10g).

4.3.3 Compaction

Mechanical compaction is one of the main reasons for porosity reduction and chemical compaction because it may reduce the porosity by dissolving the point contacts. Chemical compaction may increase the porosity by stylolite formation (Fig. 10e) and dissolution seams (Fig. 10h) (Vandeginste and John, 2013). The compressional and extensional fractures and dissolution can also be produced by tectonic activities (Tucker and Wright, 2009). Both chemical mechanical compaction is noticed in the CFm. The compactional changes are divided into two types: the mechanical compaction exhibits closer packing, contact, pores and fractures, observed in all four facies of the studied formation (Mahboubi et al., 2010); chemical compaction is clear in the CFm siliciclastic mudstone, siliciclastic wackestone and siliciclastic grainstone microfacies. Microstylolites, stylolite (Figs. 14d, e, f),

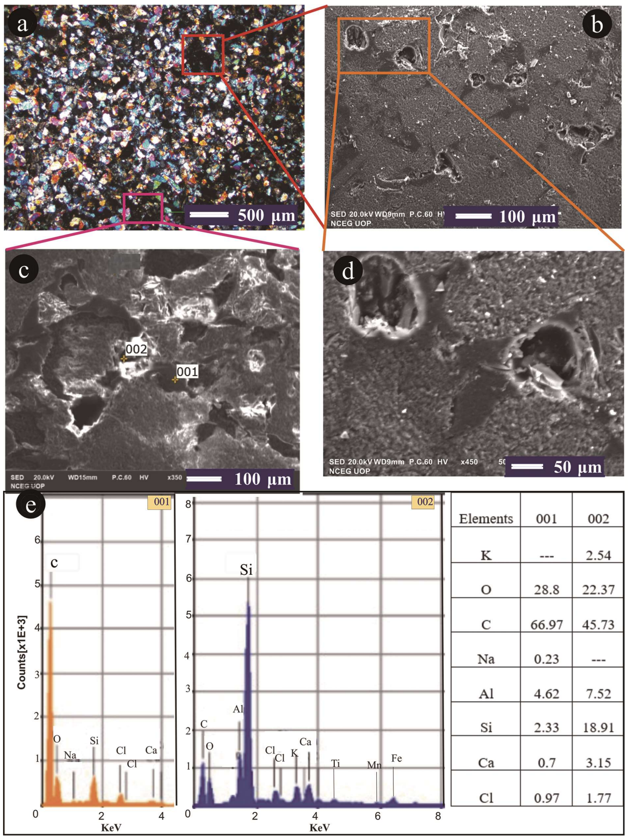

Elements	001	002
K	---	2.54
O	28.8	22.37
C	66.97	45.73
Na	0.23	---
Al	4.62	7.52
Si	2.33	18.91
Ca	0.7	3.15
Cl	0.97	1.77

Fig. 8. Photomicrograph obtained from the petrographic microscope, SEM and based microporosity and elemental composition of the selected points.

(a) Photomicrograph obtained from the petrographic microscope of the interested zone; (b–d) SEM photomicrographs showing micro porosities; (e) graph 001, 002 and table represents the elemental composition of the selected points in photomicrograph c. The number of CEM, University of Balochistan collection are given as below (a) MZK-2009-C3A; (b) MZK-2009-C3B; (c) MZK-2009-C3C; (d) MZK-2009-C3D; (e) MZK-2009-C3E.

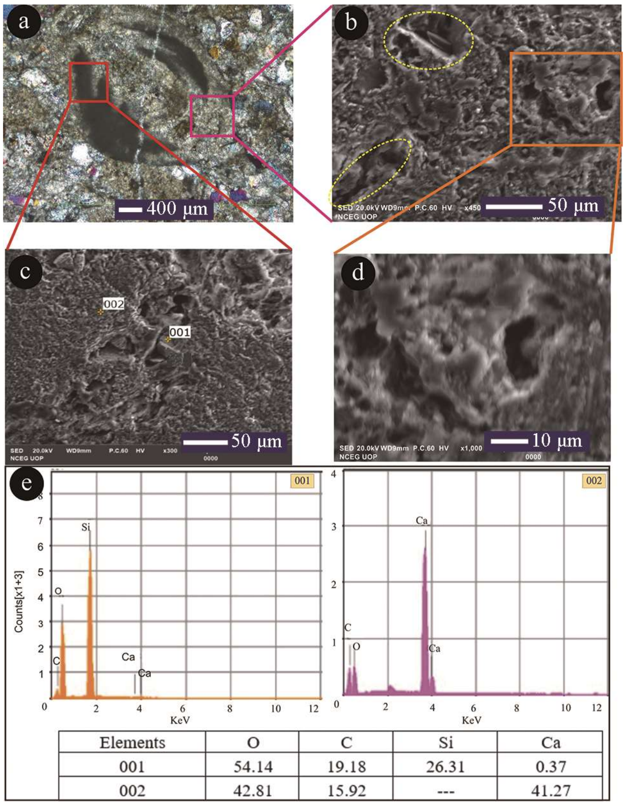

Elements	O	C	Si	Ca
001	54.14	19.18	26.31	0.37
002	42.81	15.92	---	41.27

Fig. 9. Photomicrograph obtained from the petrographic microscope, SEM and EDX to find the microporosity and elemental composition of the selected points.

(a) Photomicrograph obtained from the petrographic microscope of the interested zone; (b–d) SEM photomicrographs showing micro porosities; (e) graph 001, 002 and table represents the elemental composition of the selected points in photomicrograph c. The number of CEM, University of Balochistan collection are given as below (a) MZK-2009-C4A; (b) MZK-2009-C4B; (c) MZK-2009-C4C; (d) MZK-2009-C4D; (e) MZK-2009-C4E.

wispy seam (Fig. 14h) and solution seam (Figs. 14d, f, h, i, l) are also present.

4.3.4 Cementation

Cementation is the process in which supersaturated pore -fluids precipitate cement in the absence of any kinetic factor that prevents precipitation. The generic types of cement in carbonate rocks are high, low-Mg calcite, aragonite and dolomite, which precipitate in cavities between grains depending on the rate of carbonate supply/ precipitation and composition of pore-fluids (Tucker and Wright, 2009). Marine, meteoric and deep burial cementation signatures are observed in the CFm (Fig. 11). The identified cement types between the grains and within cavities include blocky (Figs. 11a, b, e), isopachous fibrous cement (11d), granular mosaic (Fig. 11f) and poikilotopic (Figs. 11h, i).

The isopachous fibrous calcite cement is a high Mg-calcite and shows a low rate of sedimentation (Tucker and Wright, 2009). The CFm cement diagenetic history started from this type of cement. Isopachous fibrous calcite cement is seen in the three limestone facies of CMF-1, CMF-2 and CMF-3 (Figs. 11d). It is usually formed in a marine phreatic environment as a thin cement rim (Melim et al., 2002; Vincent et al., 2007).

Blocky calcite cement is one of the most abundant types in the CFm. This type of cement is clearly seen in facies CMF-1 and CMF-2 represented by samples CN-1, CN-6, CG-2, CG-3 and CZ-4 (Figs. 11a, b, e, h) in the Siliciclastic Mudstone, Siliciclastic Wacke–Packstone and Siliciclastic Grainstone microfacies. Two phases of blocky calcite cement are found in the formation: in the first, the cement is well-established and observed in intra-skeletal pores and molds of dissolved grains (Figs. 11b, e, h). This type of diagenetic feature represents the meteoric-phreatic diagenetic realm (Khalifa et al., 2009; El Ghar et al., 2015); the second phase is where cement has filled the fractures (Fig. 11a) and shows undulatory extinction, which is an indicative feature of burial diagenesis realm (Vincent et al., 2007). The blocky calcite of these two stages is non-ferroan low magnesium calcite as indicated by the XRD results (Figs. 3, 4). The larger crystal size of the blocky calcite cement is due to uniform cementation in pores filled with supersaturated water (Tucker and Wright, 2009).

Granular mosaic cement is rare in the CFm and found in

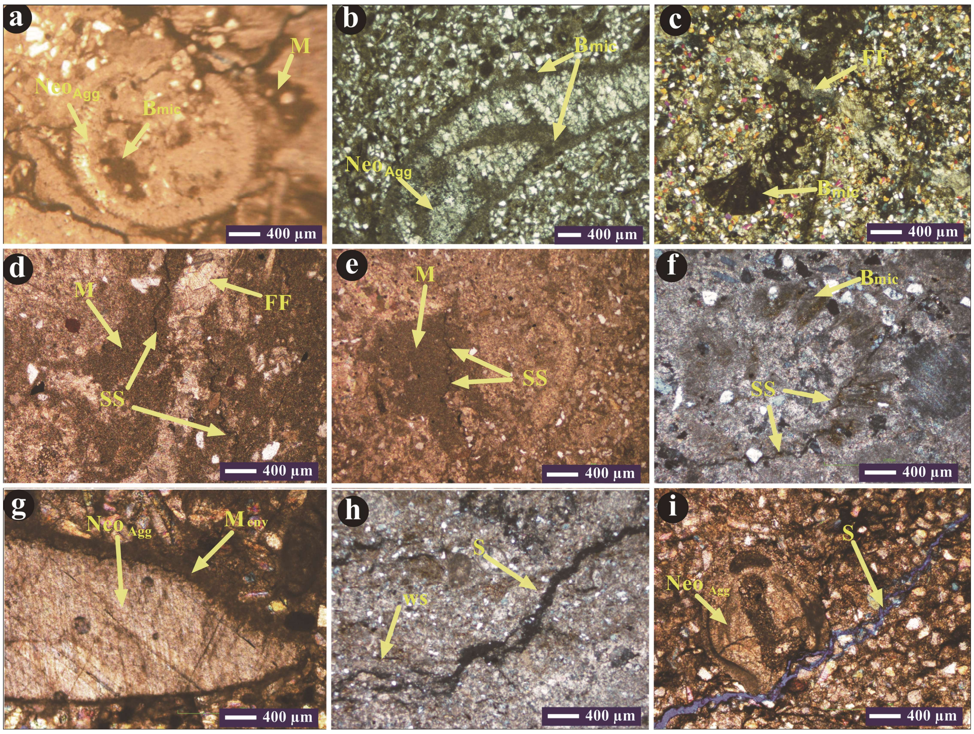

Fig. 10. Photomicrographs showing diagenetic features of the Chhidru Formation.
(a) Intense micritization (M), bioclastic micritization (B_{mic}) and shell neomorphism (Neo_{agg}) of gastropod fossil; (b) neomorphism (Neo_{Agg}) and bioclastic micritization (B_{mic}) of gastropod fossil; (c) fracture filled (FF) and bioclastic micritization (B_{mic}); (d) fracture filled (FF), intensive micritization (M) and stylolite (SS); (e) intense micritization (M) and stylolite (SS) in micrite; (f) bioclastic micritization (B_{mic}) in green algae and green algae cross cut by stylolite (SS); (g) neomorphism (Neo_{agg}) and micritic envelope (M_{env}) in bioclasts; (h) solution seam (S) and to left side, converted into wispy seam (WS); (i) neomorphism (New_{Agg}) in bioclast and solution seam (S) highlighted by blue dye.

sample CZ-12 of the Siliciclastic Wackestone and Sandstone microfacies. (Fig. 11f). The granular mosaic cement-filled pores between skeletal and siliciclastic grains having sub-hederal crystal form precipitated in a meteoric phreatic environment (Mahboubi et al., 2010; El Ghar et al., 2015), and is usually associated with green algae and skeletal allochems.

The poikilotopic cement occurs between the siliciclastic grains and bioclasts in the CFm (Figs. 11h, i). This cement usually develops large crystals due to slow growth in a relatively deep burial diagenetic environment, but here in the CFm, the crystal size is small, which reflects the availability of less space for cement precipitation. The poikilotopic cement is formed in a deep burial diagenetic environment (Ahr, 2011). The CFm poikilotopic calcite (Fig. 11i) formed in the late stage of cementation, as confirmed by textural relationship.

4.3.5 Dissolution

Undersaturated pore fluids and burial pressure can cause dissolution of carbonate sediments and cements in limestone. The process of dissolution is mainly controlled by mineralogy, pore-fluid saturation and burial pressure (Tucker and Wright, 2009). The vuggs and cavities are formed as a result of a dissolution process that can take place soon after deposition as well as after uplift of rocks (Tucker and Wright, 2009). Dissolution has affected rocks throughout the CFm, but is presented in the wackestone and packstone facies. There are two stages of dissolution recognized in the CFm: firstly, dissolution of metastable minerals and intergranular cements occurred, which is a distinctive feature of a marine meteoric environment. This dissolution is observed in all four CFm facies. It occurs when the metastable grains and intergranular cement are dissolved due to undersaturated pore fluids and, as a result, biomoldic porosity is created (Fig. 14), which is later filled partially or completely by blocky calcite cement (Fig. 11a); the latest stage of dissolution is represented by destruction of intergranular microcrystalline cement and generation of the microporosity (Figs. 11k, l). In the CFm mud-supported microfacies, micrization has been affected by this type of dissolution (Figs. 6–9).

4.3.6 Fractures

Fractures are the discontinuities produced by the process of mechanical diagenesis and deformational events (Nelson, 2001). The most popular reservoir in the world are brittle-fractured carbonate rocks, which are formed at a shallow burial pressure depth (Roehl and Choquette, 2012). Petrographic studies show that the CFm samples with a relatively high clastic content are affected by fracturing (Fig. 11). Since the samples were collected from the hanging wall of the Salt Range Thrust (SRT), these fractures are associated with the deformation of the SRT hanging wall strata during fault translation and fold development (Figs. 11g, j). The majority of these fractures are filled with calcite (Figs. 14c, d) while a few are

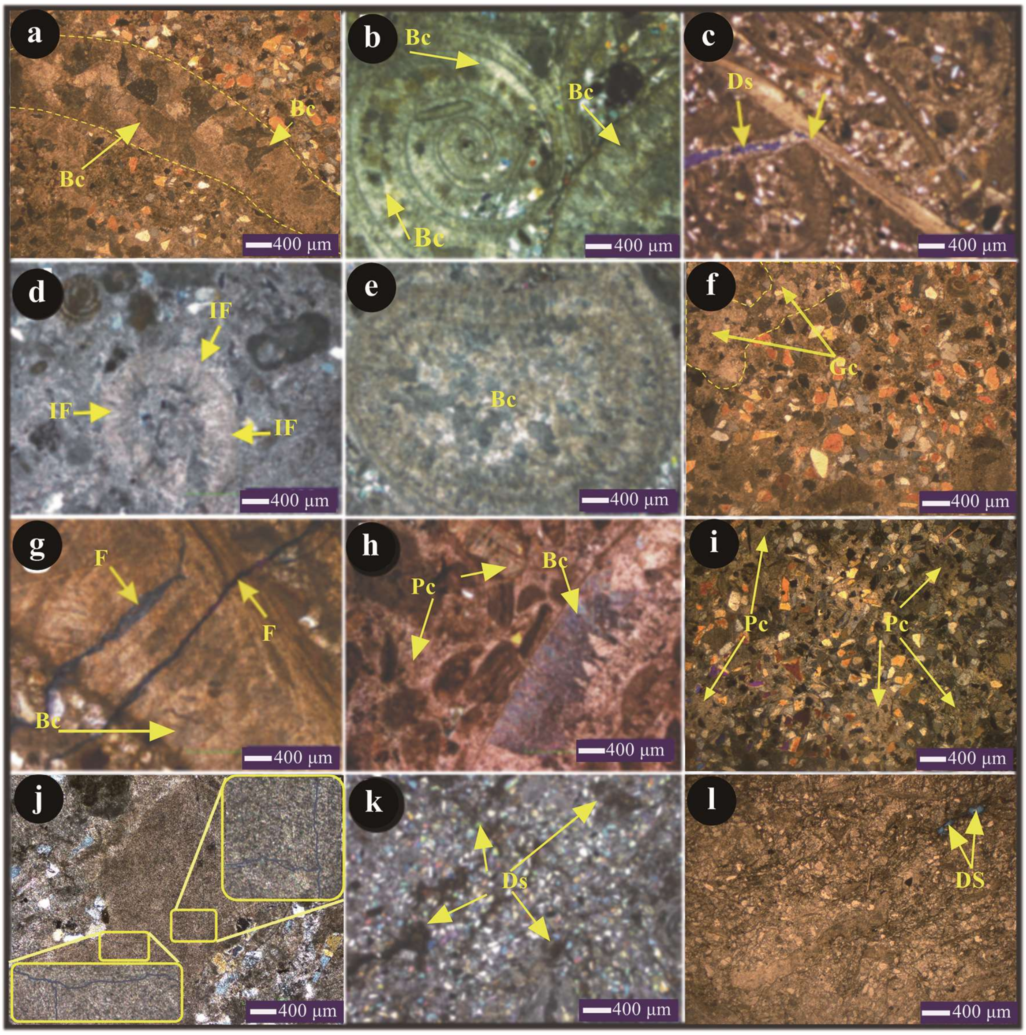

Fig. 11. Photomicrographs of diagenetic features in the Chhidru Formation.
(a) Blocky-type cement precipitated after dissolution of bioclasts; (b) gastropod fossil neomorphosed to blocky cement; (c) continuity of dissolution of bioclast from the bottom and converted to dissolution seam on the left side; (d) outer edge of echinoderm plate covered by isopachous fibrous calcite cement; (e) whole echinoderm plate neomorphosed to blocky cement; crystal size is large in the center and decreases towards the margin; (f) granular mosaic cement observed in Zaluch Gorge Section; (g) chronological order of features noticed for aggrading type of neomorphism blocky cement (b) in bioclast followed by brittle fracturing; (h) blocky calcite cement in bioclast and to left top is poikilotopic cement; (i) poikilotopic type of calcite cement; (j) fractured rock; (k) and (l) show dissolution of metastable minerals.

unfilled (Fig. 14g).

4.4 Diagenetic environments

The signature of the metastable and stable sediment deposition, their lithification and other diagenetic phases are preserved in almost every rock until the process of the weathering and metamorphism demolish the rock strata (Esrafili-Dizaji and Rahimpour-Bonab, 2010). The transformation of the metastable sediments to stable minerals can take place in different environments from marine depositional through meteoric to burial diagenetic (Fig. 12; Tucker and Wright, 2009). The CFm has been modified in different diagenetic environments (Fig. 12).

4.4.1 Marine diagenetic environment

The dominant composition of the CFm mudstone, siliciclastic wacke–packstone and grainstone microfacies is Mg-calcite derived from bryozoan fossils, aragonite from bivalves and gastropod and clastic grains that indicate a shallow marine environment of deposition (Ahmad et al., 2015). In phreatic marine settings, pores are filled by marine water and shallow marine diagenetic alteration can occur (Flügel, 2010). The diagenesis of the studied formation started from a marine to a submarine environment, which is indicated by the micritization, existence of deposited minerals and bioclastic grains and non-ferroan isopachous fringes cement (Figs. 12, 13). The micritization takes place at the sediment–water interface and is induced by the endolithic algae, fungi, and bacteria (Adams and MacKenzie, 1998). The micritization and isopachous fibrous calcite cements observed in the CFm are noticeable diagenetic features of a marine environment (Figs. 10, 11).

4.4.2 Meteoric environment

A meteoric diagenetic environment is the most

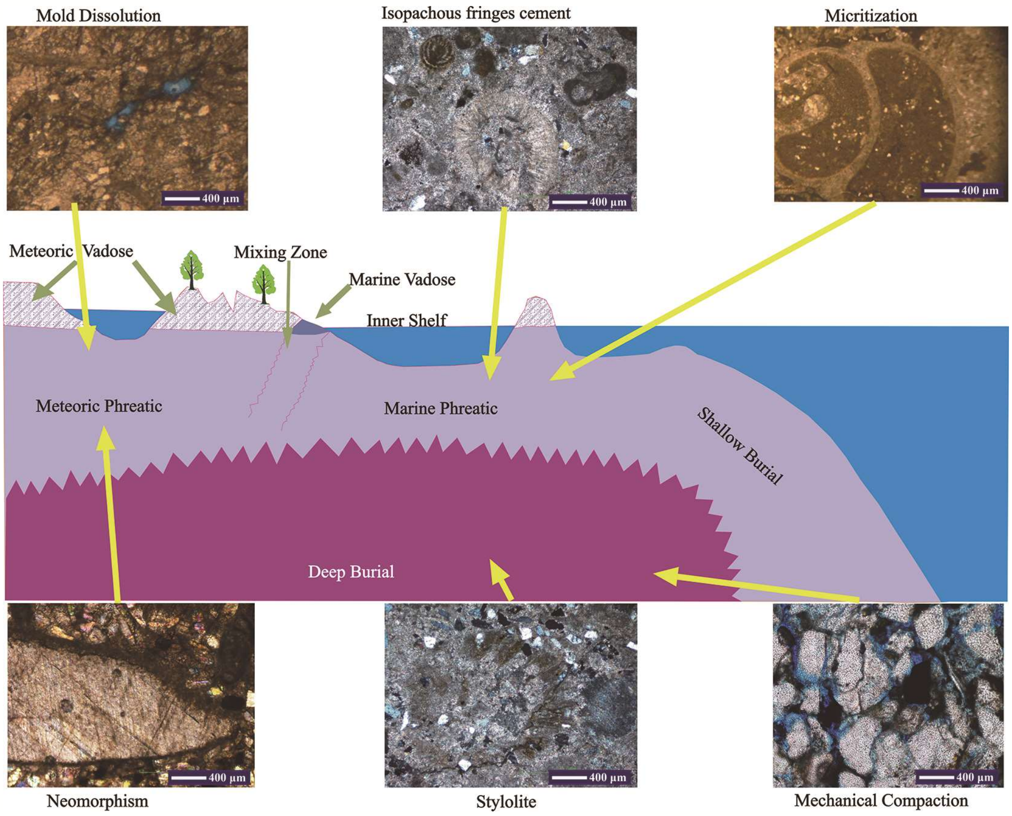

Fig. 12. Diagenetic model of the Chhidru Formation representing different diagenetic stages, ranging from shallow burial, micritization and cementation, medium burial, dissolution, deep burial, neomorphism, stylolitization and mechanical compaction.

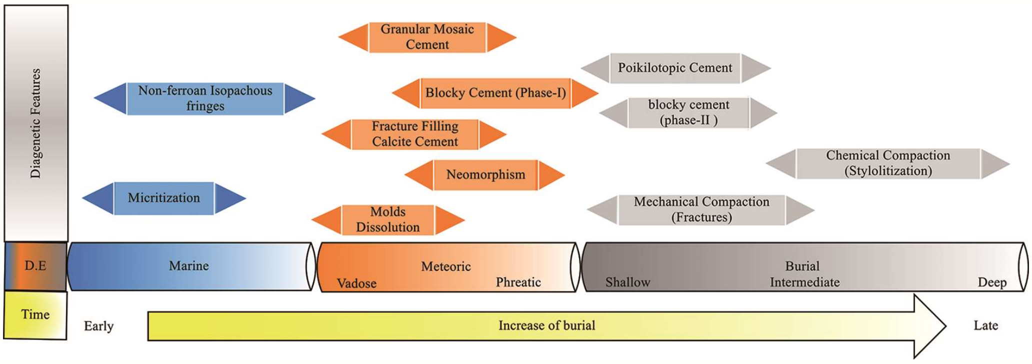

Fig. 13. Paragenetic sequence of the Chhidru Formation showing different diagenetic processes with their respective environment.

D.E.–diagenetic environment.

important one to enhance the reservoir properties of carbonate rocks and can be divided into vadose and phreatic zones (Tucker and Wright, 2009). The diagenetic features of the water-filled phreatic zone can be differentiated from the water- and air-dominated vadose zones. The phreatic zone cement is indicated by the growth of larger crystals towards the center of the pore and low Fe content (Tucker and Wright, 2009).

The neomorphism of the metastable minerals, mold dissolution, initial stage blocky cement (Phase-I) and granular mosaic cement are indications of the meteoric phreatic and vadose diagenetic environments (Mahboubi et al., 2010; El Ghar et al., 2015). The aggrading neomorphic alteration, ranging in size from micro-spar to blocky cement, effects all the CFm carbonate lithofacies (Figs. 10a, b, i, 11g), suggesting meteoric phreatic environments (Fig. 12).

4.4.3 Burial diagenetic environment

Burial diagenetic signatures such as mechanical and chemical compaction have been recognized. The most pronounced features in the CFm are chemical compaction, as indicated by stylolites. Mechanical compaction is rarely noticed; however, it is extensively preserved in the quartz

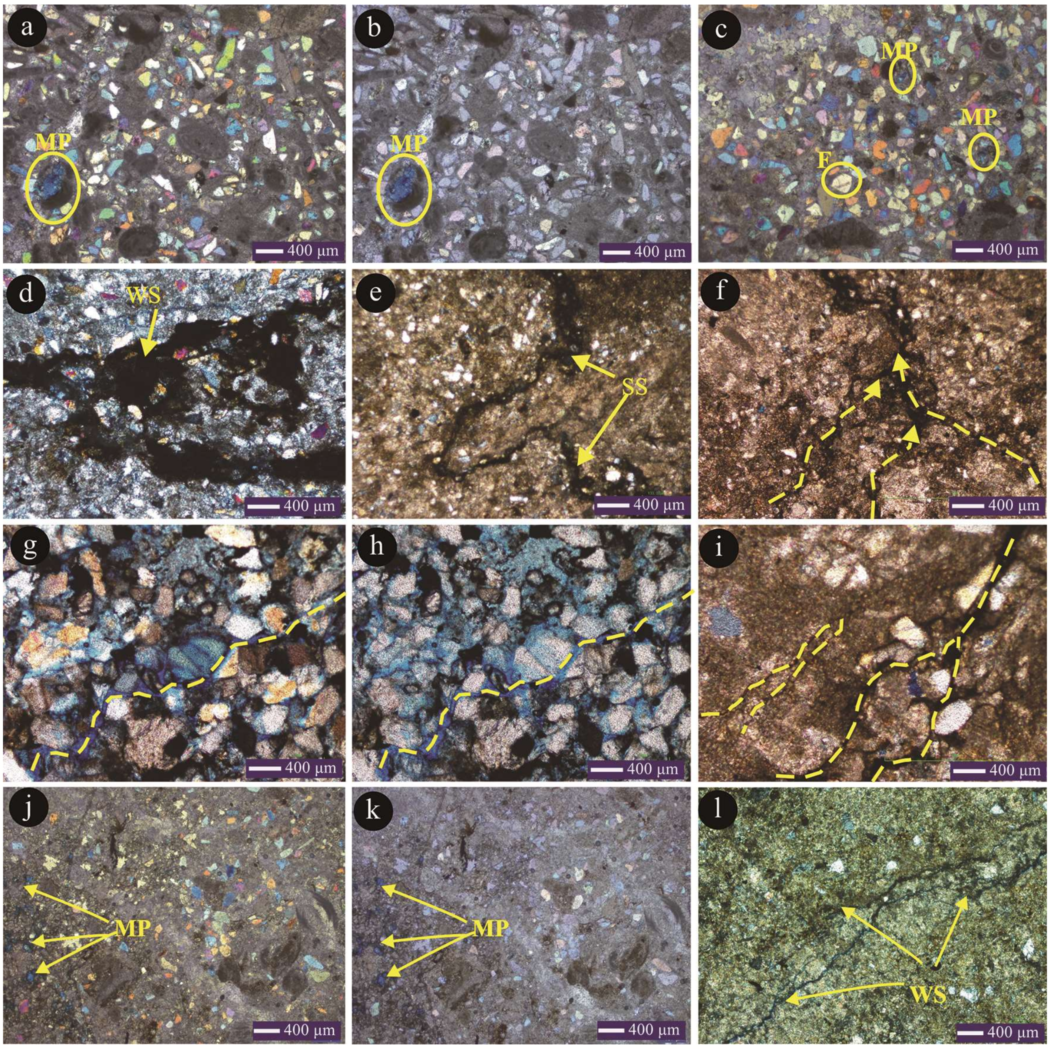

Fig. 14. Photomicrographs showing the reservoir quality of the Chhidru Formation.
(a–b) Dissolution in bioclast forming moldic type of pore (MP); (c) moldic type (MP) of pores and fracture created in pre-existing minerals; (d) wispy type (WS) of dissolution in chemical compaction; (e) high-amplitude stylolite (SS) formed due to chemical compaction in the siliciclastic grain stone facies; (f) wispy type of solution seam formed in siliciclastic grain stone facies; (g–h) moldic porosity that may act for good effective porosity; (i) siliciclastic grain stone facies effected by wispy type solution; (j–k) moldic porosity (MP) in left bottom corner; (l) wispy (WS) type of porosity formed in siliciclastic wacke-stone facies.

wacke sandstone facies. The phase-II blocky calcite cement (Fig. 10a), which shows undulatory extinction and precipitated poikilotopic cement (Fig. 11i) is the diagenetic cement type of the burial environment (Ahr, 2011) present in the CFm.

4.5 Paragenetic sequence of diagenesis

The paragenetic sequence of the CFm includes marine, marine-meteoric, meteoric and burial diagenetic environments (Fig. 13). The CFm sequence starts from micritization and non-ferroan isopachous fringes type of cement formed in a marine phreatic environment. The regular non-destroyed micrite envelopes imply that micritization occurred prior to the onset of compaction. Mold dissolution, fracture-filled calcite cement and granular mosaic cement are formed, respectively, in a meteoric vadose diagenetic environment. The next diagenetic phase was neomorphism of metastable minerals and blocky cement (i.e. Phase-I) in a meteoric phreatic diagenetic environment. Once the burial increased to shallow to intermediate, mechanical compaction, blocky cement (i.e. Phase-II) and poikilotopic cement formed and the chemical compaction (i.e. stylolitization) are the last diagenetic signatures observed in the CFm formed in a deep burial environment (Figs. 12, 13).

4.6 Diagenetic controls on reservoir quality in the Chhidru Formation

In contrast to siliciclastic rocks, carbonates seldom possess any dominant primary porosity, particularly carbonate lithofacies that contain micritic mud that infills both intergranular and intragranular pore spaces. The reservoir properties of carbonate rocks are commonly credited to secondary diagenetic processes (Tucker and Wright, 2009; Amel et al., 2015). Such porosity and permeability enhancing processes include dissolution, fracturing, and dolomitizaation.

The formation/CFm is primarily dominated by lithifying

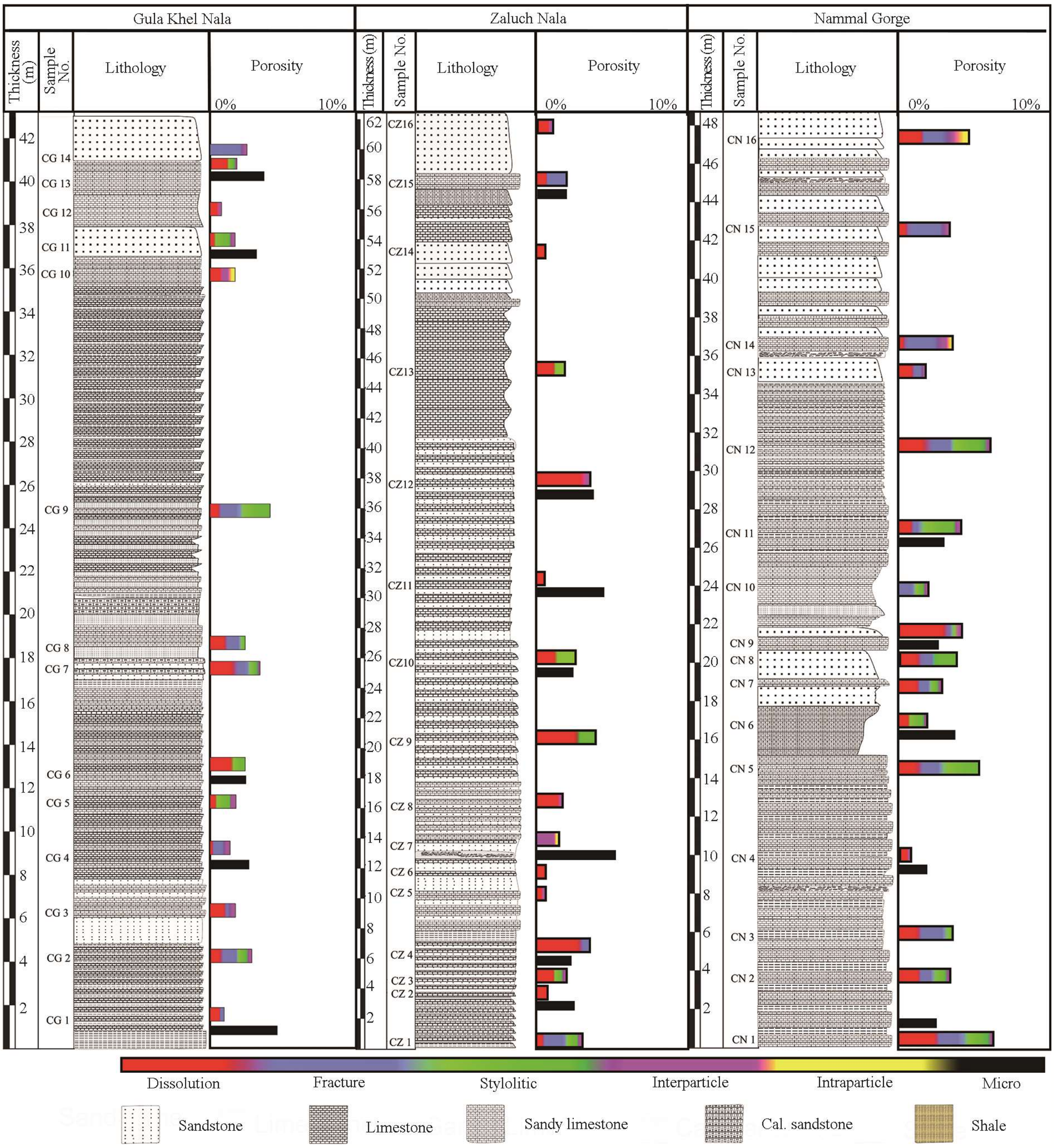

Fig. 15. The stratigraphic column and calculated porosity of the Chhidru Formation at Gula Khel Gorge, Zaluch Gorge and Nammal Gorge, Pakistan.

The black color shows the microporosity estimated from the SEM, photomicrograph; other colors represent dissolution (red), fracture (blue), stylolitic (orange), interparticle (violet), and intraparticle (yellow) porosities. Sample's locations and number of are shown from three sections in the Chiddru Formation: Nammal Gorge, Zaluch Nala and Gula Khel Nala.

cement and inter/intragranular porosity ascribed probably to the dissolution of cement (Fig. 14). The secondary porosity of fractures, stylolites and moldic pores mostly related to dissolution of cements are present (Figs. 10, 11). Most of the primary porosity of intergranular and intragranular is probably destroyed by cementation. Diagenetic processes are mainly responsible for the generation of the secondary porosity. The predominant type of porosity is dissolution, fracture and stylolites, but inter-particle and intra-particle porosity is also observed in some thin sections (Fig 15). The dissolution and cementation are observed and confirmed by SEM-EDX. The EDX graph further displays the elemental composition of silicon (Si), oxygen (O) and carbon (C) at point 001 (i.e., pink curve) and point 002 (i.e., blue curve) (Figs. 6–9).

Porosity was calculated through image processing using Jmicrovision Openware Software (Fig. 15). The porosity of the overall CFm is moderate to very low, but CMF-4 facies exhibited moderate to high porosity in all three-studied sections (Figs. 2, 15). The average porosity of the CMF-2, CMF-3 and CMF-1 is 2.65%, 3.25% and 3.96%, respectively. In the moderate to high porosity zones, CMF -4, the average porosity is 7.14%.

The microporosity investigated through SEM of the selected samples from all facies of the three sections also indicated low porosity in facies CMF-1, CMF-2, CMF-3, but promising porosities in the CMF-4 facies (Figs. 6–9). The CMF-1, CMF-2 and CMF-3 facies show average microporosity of 4.8%, 5.0% and 5.3% respectively, whereas the CMF-4 facies show higher than average microporosity of 10.7%.

4.7 Porosity model

Significant reservoir properties, i.e., porosity and permeability, depend on the depositional fabric, such as composition, texture and fabric of the sediment. The derivative mode of porosity is divided into three types: depositional processes, diagenetic routes, and mechanical fracturing (Ahr, 2011). A triangular diagram is used to plot these three-porosity modes; Siliciclastic Mudstone and Siliciclastic Wacke to Sandstone are placed into diagenetic-dominated and fracture-dominated ends, respectively, whereas the porosities of Siliciclastic Wackestone and Siliciclastic Grainstone facies are controlled by both, diagenesis and fracturing (Fig. 16).

The depositional characters are sedimentary structures, texture and mineral composition of the original deposited rock and the porosity created by the processes of re-precipitation, dissolution and replacement is termed 'diagenetic porosity'. This type of porosity can change mineralogical composition, texture and fabric of the original deposited rock. Diagenetic porosity may be purely diagenetic or depositional and fracture porosity will be enhanced by the diagenetic process. This diagenesis can enhance or reduce the porosity of the rock.

Nelson (2001) classified fractures as surface, contractional, regional, tectonic and morphological fractures. Morphological fractures are further subdivided into open, deformed, mineral-filled and vuggy fractures. Most importantly, the matrix pores contribute to the fracture porosity, because if matrix pores are very low or not connected with fracturing then it these pores may be useless. Open, mineral-filled and vuggy fractures are observed in all CFm four facies (Figs. 11, 16).

4.7.1 Diagenetically enhanced porosity

Diagenetic agents of recrystallization, dissolution and replacement of diagenetic process enhance porosity (Walter, 1983). The diagenetic process of neomorphism and chemical compaction have enhanced the microporosity of the CFm. The dissolution process is a diagenetic process of unconformities, soil regions, karst topography and exposed places (Ahr, 2011). Replacement normally reduces the porosity of the carbonate rock, but microcrystalline microporosity is observed in samples examined under the SEM (Figs. 6, 9).

4.7.2 Diagenetically reduced porosity

Cementation, micritization and compaction along with neomorphism (recrystallization and replacement) are the main diagenetic agents of porosity reduction. Compaction takes place as a result of overburden and tectonic activities, and may create stylolites, which can increase in mud-supported rock and normally stops the flow in a reservoir, but post-stylolitic diagenesis can enhance the reservoir characteristic (Dawson, 1988). A few stylolites in the siliciclastic mud stone facies of the CFm are limited in lateral extension (Fig. 10d) and may have reduced the reservoir quality. Neomorphic recrystallization reduces the porosity but neomorphic stabilization (normally Mg-calcite and aragonite stabilization) can improve the porosity. The change of original mineral and fabric in the replacement process can drop the reservoir properties, i.e., porosity and permeability, of the rock. From depositional site to deep burial environment, cementation can take place in all diagenetic environments.

The paragenetic sequences of the studied rocks allow to decipher the succession of events and their effects on the porosity evolution through time. The first cement that reduced porosity is the fibrous isopachous marine type. As sediments were gradually buried, fracture generation was accompanied by formation of poikilotopic cement on the one hand and by dissolution on the other.

5 Petroleum Prospects of the Chhidru Formation

The oil potential of the CFm can possibly be fed by several underlying source rocks, primarily the Precambrian Salt Range Formation, which is a proven and potential source rock in the Upper Indus Basin (Kadri, 1995). The second source for the CFm is the Cambrian Khewra, Kussak, Jutana and Khisor formations, which contain shales rich in organic matter; certain evidence has already been reported reflecting hydrocarbon generation in the Cambrian shales (Kadri, 1995). Moreover, the shale of the underlying Early Permian Dandot and Sardhai formations and limestone and shales of the Zaluch Group also qualify as source rock parameters in several locations

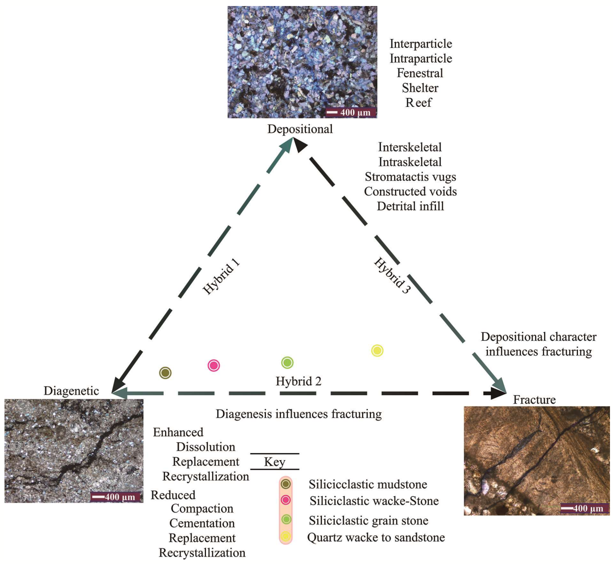

Fig. 16. Genetic classification model for the Chhidru Formation, showing the effect of depositional, diagenetic and deformational agents.

in the Trans-Indus ranges (Kadri, 1995). The CFm shows alternate beds of sandstone and limestone and shales, all of which show the potential of reservoir compartmentalization (Ahmad et al., 2015). In terms of seal rocks, the upper Triassic Mianwali, Tredian and Kingriali formations have some shale members, which can act as a seal for the CFm (Kadri, 1995). Additionally, the CFm top is marked by an unconformity, where there is probability for the development of a cemented surface and hence for the formation of a stratigraphic trap (Farid et al., 2018).

Structurally, the Potwar Plateau has experienced thin-skinned deformation and hence presents mostly structural traps (Kadri, 1995). The stratigraphic level of the Permian CFm has been dissected by different faults (Farid et al., 2018). Moreover, the interval of Permian succession on the surface is also undulated but very gently and, as such, faults can enhance the overall porosity and permeability of the CFm in the subsurface (Farid et al., 2018).

6 Discussion on Regional Correlation

6.1 Respective potential facies

During late Permian time, due to a similar geographic location of the Arabian and Indian platforms, an analogous depositional setting was developed (Jan et al., 2009), from which the Upper Permian CFm and the upper part of Khuff Formation developed similar facies. Similar to the CFm, the Khuff Formation facies are alternate carbonates, sandstone, and shale (Al-Aswad, 1997). The extensive Permian platform of Arabia shows an increasing siliciclastic content towards the depositional shelf in the south. In Pakistan, the shelf geometry shows a deepening towards the north. There is a close similarity between facies of the Indian and Arabian upper Khuff Formation. In the Khuff Formation, the Khuff-C Member, which is mainly grainstone and siliciclastic facies, is an excellent reservoir (Alsharhan and Nairn, 1994). In the CFm, the same grainstone–packstone and sandstone facies are potential reservoir facies.

6.2 Reservoir comparison

Reservoir properties like porosity and permeability show that the Khuff and Dalan formations in Persian/Iranian basins, show an average porosity range of >10% in offshore fields and <4% in inner Persian/Iranian basins. The porosity trends show a prominent drop in average porosity toward the basin (Esrafili-Dizaji, 2010). In the Permian succession, the porosity values of the Arabian Plate (Khuff Formation) are higher than in Persian basins (Dalan Formation). As per permeability, the Permian of Iran, Qatar and Bahrain show good results compared to Arabian successions. Both porosity and permeability of the Khuff Formation of the UAE are insignificant (Esrafili-Dizaji, 2010).

In comparison, the porosity of the CFm (i.e., 0–15%) shows variable results in different parts of the basin. The CFm reservoir properties increase to north of the basin. In overall comparison, the Arabian Khuff and Persian/Iranian Dalan formations share the same reservoir properties with the CFm.

6.3 Diagenesis sequences and porosity variation

Diagenesis greatly affected the reservoir properties of the Khuff Formation on the Arabian plate (Moradpour et al., 2008). In the early stage of diagenesis, deposition occurred in an open marine setting. Different diagenetic processes such as micritization, cementation and early stage dolomitization are common in the Khuff Formation whereas the CFm hosted cementation, compaction and neomorphism. At this stage, the primary porosity of both formations was destroyed.

In a shallow marine diagenetic setting, different processes like drusy and blocky cement, dissolution, neomorphism and aragonite stabilization are key elements of meteoric diagenesis in the Khuff Formation. In the CFm, blocky cements are present in almost all carbonates. Poikilotopic cement occurs very limitedly between grains of quartz.

In a deep burial late stage, porosity by means of fractures produced represent the main reservoir assets. Dissolution and dolomitization are the second main porosity factors at this stage. Compaction and cementation are involved in decreasing porosity at this stage, and, produces secondary porosity in the Khuff Formation.

According to Ehrenberg et al. (2007), cementation and compaction greatly affected the limestone and dolomitic facies. The secondary porosity is also affected by anhydrite. In the Khuff Formation, inter-particle, inter-crystalline, fenestral and moldic porosities are the main type of porosities (Enos and Sawatsky, 1981; Schmoker and Halley, 1982). The porosity in the CFm is also secondarily formed due to diagenetic processes like dissolution, stylolites and fractures. The predominant type of porosity is dissolution, fracture and stylolitic, but inter-particle and intra-particle porosity is observed. The diagenetic events destroyed primary porosity and produced secondary porosity.

7 Conclusions

The Chhidru Formation (CFm) consists of four depositional facies, i.e. siliciclastic mudstone microfacies (CMF-1), siliciclastic wacke–packstone microfacies (CMF -2), siliciclastic grainstone microfacies (CMF-3) and quartz-wacke to sandstone microfacies (CMF-4). The CMF-4 and CMF-3 facies show some potential reservoir zones, whereas CMF-1 and CMF-2 represent poor zones for reservoir potential.

The formation is significantly influenced by diagenetic processes that have obliterated the reservoir properties, particularly in carbonate microfacies CMF-1, CMF-2 and CMF-3. The major diagenetic agents involved are micritization, cementation, dissolution, neomorphism, compaction and fracturing. Diagenetic processes of marine, meteoric and burial environments, such as cementation, compaction and neomorphism have destroyed the primary porosity.

The porosity in the CFm is mainly secondary, formed due to diagenetic processes like dissolution, stylolites and fractures. The blocky type of cement (phase-I and II) is observed in almost all carbonate samples of the CFm, and forms what is the main cause of low porosity in the carbonate facies. Poikilotopic cement occurs very limitedly between grains of quartz and other minerals. The predominant type of porosity is dissolution, fracture and stylolitic, but inter-particle and intra-particle porosity are observed in some intervals, mostly in CMF-4 facies. The overall average porosity is 2% to 7% in all three studied sections of the CFm but the CMF-4 facies has the highest porosity. The CMF-2 facies has lowest porosity in the Zaluch Gorge and Nammal Gorge sections with an average of 2% to 3%, but in the Gula Khel section, CMF-2 facies porosity is better than CMF-3 facies. In the Gula Khel Section the lowest porosity is in CMF-3 facies having average of 1.8% to 2.7%. In terms of intra-formation comparison, the CMF-1 facies has an average porosity of 3% to 4.5%. Among the three studied sections, the Nammal Gorge Section porosity is highest, and the Gula Khel Gorge Section has lowest porosity. The microporosity results show the highest porosity in CMF-4 facies and lowest porosity in CMF-1 and CMF-2 facies.

Overall, the Chhidru Formation has a low porosity except in one sandy facies, CMF-4. Diagenesis has destroyed primary porosity but produced some secondary porosity.

Acknowledgements

Two anonymous reviewers and editors were thanked for their help in improving this manuscript. Dr. Susan Turner (Brisbane) assisted with English language.

Manuscript received May 26, 2020
accepted Mar. 10, 2021
associate EIC: ZHANG Shuichang
edited by Susan TURNER and FANG Xiang

References

Adams, A.E., and Mackenzie, W.S., 1998. A colour Atlas of carbonate sediments and rocks under the-microscope. Boca Raton: Manson Publishing, Florida, United States.

Aamir, A., Matee, U., Matloob, H., Bhatti, A.S., and Khaista, R., 2017. Estimation of the shale oil/gas potential of a Paleocene–Eocene succession: A case study from the Meyal area, Potwar Basin, Pakistan. Acta Geologica Sinica (English Edition), 91 (6): 2180–2199.

Ahmad, S., Ullah, M., Ullah S., Khan, S., Khan, Y., Jan, I.U., Rehman, K., Mohibullah, M., Attaullah, and Jan, S., 2018. Stratigraphic and Paleoclimatic Reconstruction of the Upper Carboniferous-Lower Permian strata from the Southern Gondwanaland remnants in Pakistan. Stratigraphy, 15(2): 69–90.

Ahmed, K.A., Khan, S., Sultan, M., Umair, B.N., Ullah, K., and Mu'ayyad, A.H., 2019. Precise seismic substructural model of the eocene chorgali limestone in the Turkwal oil field, Central Potwar, Pakistan. Acta Geologica Sinica (English Edition), 93 (6): 1711–1720.

Ahmad, S., Waqas, M., Khan, S. S., Swati, F., Azhar, M., Jan, I. U., Ali, F., Yaqoob, M., Sadiq, A., and Khan, S., 2015. Facies analysis and dynamic depositional modelling of the Upper Permian Chhidru Formation, Salt Range, Upper Indus Basin, Pakistan. Journal of Himalayan Earth Science, 48(1): 64–80.

Ahr, W.M., 2011. Geology of carbonate reservoirs: The identification, description and characterization of hydrocarbon reservoirs in carbonate rocks, Hoboken: John Wiley and Sons, New Jersey, United States. DOI: 10.1002/9780470370650.

Al-Aswad, A., 1997. Stratigraphy, sedimentary environment and depositional evolution of the Khuff Formation in south-central Saudi Arabia. Journal of Petroleum Geology, 20(3): 307–326.

Alsharhan, A., and Nairn, A., 1994. The Late Permian carbonates (Khuff Formation) in the western Arabian Gulf: Its hydrocarbon parameters and paleogeographical aspects. Carbonates and Evaporates, 9(2): 132.

Amel, H., Jafarian, A., Husinec, A., Koeshidayatullah, A., and Swennen, R., 2015. Microfacies, depositional environment and diagenetic evolution controls on the reservoir quality of the Permian Upper Dalan Formation, Kish Gas Field, Zagros Basin. Marine and Petroleum Geology, 67: 57–71.

Angiolini, L., Balini, M., Garzanti, E., Nicora, A., and Tintori, A., 2003. Gondwanan deglaciation and opening of Neotethys: The Al Khlata and Saiwan formations of interior Oman. Palaeogeography, Palaeoclimatology, Palaeoecology, 196: 99–123.

Awais, M., Hanif, M., Ishaq, M., and Irfan, U.J., 2020. An integrated approach to evaluate dolomite in the Eocene Chorgali Formation, Khair-e-Murat Range, Pakistan: Implications for Reservoir Geology. Journal of Himalayan Earth Sciences, 53(1): 12–23.

Badiozamani, K., 1973. The Dorag dolomitization model-application to the Middle Ordovician of Wisconson. Journal of Sedimentary Petrology, 43: 965–984.

Baiyegunhi, C., Liu, K., and Gwavav, O., 2017. Diagenesis and Reservoir Properties of the Permian Ecca Group Sandstones and Mudrocks in the Eastern Cape Province, South Africa. Minerals, 7: 88.

Bjorlykke, K., and Jahren, J., 2012. Open or closed geochemical systems during diagenesis in sedimentary basins: Constraints on mass transfer during diagenesis and the prediction of porosity in sandstone and carbonate reservoirs. AAPG Bulletin, 96(12): 2193–2214.

Dawson, W.C., 1988. Stylolite porosity in carbonate reservoirs. Tulsa: American Association of Petroleum Geologists, Oklahoma, USA.

Duan, Y., Xie, J., Li, B., Wang, M., Zhang, T., and Zhou, Y., 2020. Lithology identification and reservoir characteristics of the mixed siliciclastic-carbonate rocks of the lower third member of the Shahejie Formation in the south of the Laizhouwan Sag, Bohai Bay Basin, China. Carbonates and Evaporites, 35: 55.

Dunoyer de Segonzac, G., 1970. The transformation of clay minerals during diagenesis and low grade metamorphism: A review. Sedimentology, 15: 281–346.

Edgell, H.S., 1977. The Permian system as an oil and gas reservoir in Iran, Iraq and Arabia. Proceedings of the Second Iranian Geological Symposium, Tehran, Iran, 161–201.

Ehrenberg, S., Nadeau, P., and Aqrawi, A., 2007. A comparison of Khuff and Arab reservoir potential throughout the Middle East. AAPG Bulletin, 91(3): 275–286.

Enos, P., and Sawatsky, L., 1981. Pore networks in Holocene carbonate sediments. Journal of Sedimentary Research, 51(3): 961–985.

Egeran, N., and Tasman, C., 1951. On the oil possibilities of Turkey with special reference to the Raman field. 3rd World Petroleum Congress, The Hague, Netherlands, Paper number WPC-4012.

El Ghar, M.S.A., Khalifa, M., and Hussein, A., 2015. Carbonate diagenesis of the mixed clastic–carbonate Galala Formation, North Eastern Desert, Egypt. Arabian Journal of Geosciences, 8: 2551–2565.

Esrafili-Dizaji, B., and Rahimpour-Bonab, H., 2010. Effects of depositional and diagenetic characteristics on carbonate reservoir quality: A case study from the South Pars gas field in the Persian Gulf. Petroleum Geoscience, 15(4): 325–344.

Farid, A., Khalid, P., Ali, M.Y. Iqbal, M.A., and Jadoon, K.Z., 2018. Seismic stratigraphy of the Mianwali and Bannu depressions, north-western Indus foreland basin. International Journal of Earth Sciences, 107: 1557–1578.

Flügel, E., 2010. Microfacies of carbonate rocks: Analysis, interpretation and application (second edition). Tulsa: Springer, United States, 1–84.

Folk, R.L., 1959. Practical petrographic classification of limestones. AAPG Bulletin, 43: 1–38.

Ghani, M., 2017. Three dimensional stratigraphic facies and reservoir properties modelling of Permian strata, Upper Indus

Basin, Pakistan (Unpublished MS Thesis), University of Peshawar, Pakistan.

Gee, E.R., 1989. Overview of the geology and structure of the Salt Range, with observations on related areas of northern Pakistan. Geological Society of America Special Paper, 232: 95–112.

Györi, O., Haas, J., Hips, K., Lukockzki, G., Budai, T., Demeny, A., and Szocs, E., 2020. Dolomitization of shallow-water, mixed silicilastic-carbonate sequences: The Lower Triassic ramp succession of the Transdanubian Range, Hungary. Sedimentary Geology, 395: 105549.

Hendry, J.P., Wilkinson, M., Fallick, A.E., Haszeldinw, R.S., 2000. Ankerite cementation in deeply buried Jurassic sandstones reservoirs of the Central North Sea. Journal of Sedimentary Research. 70: 227–239.

Jadoon, I.A.K., 1991. Thin-skinned tectonics on continent/ocean transitional crust, Sulaiman Range, Pakistan (Ph.D. thesis). Eugene: Oregon State University, USA.

Jafarian, A., Javanbakht, M., Koeshidayatullah, A., Pimtel, N., Salad Hersi, O., Yahyaei, A., and Beigi, M., 2018. Paleoenvironmental, diagenetic, and eustatic controls on Permo-Triassic carbonate-evaporite reservoir quality, Upper Dalan and Kangan formations, Lavan Gas Field, Zagros Basin. Geological Journal, 53: 1442–1457.

Jan, I.U., and Stephenson, M.H., 2011. Palynology and correlation of the Upper Pennsylvanian Tobra Formation from Zaluch Nala, Salt Range, Pakistan. Palynology, 35: 212–225.

Jan, I.U., Stephenson, M.H., and Khan, F.R., 2009. Palynostratigraphic correlation of the Sardhai Formation (Permian) of Pakistan. Review of Palaeobotany and Palynology, 158: 72–82.

Kadri, I.B., 1995. Petroleum geology of Pakistan. Pakistan Petroleum Limited, Karachi.

Khan, Z., Ahmad, A.H.M., Sachan, H.K., and Quasim, M.A., 2018. The effects of diagenesis on the reservoir characters in ridge sandstone of Jurassic Jumara dome, Kachchh, Western India. Journal Geological Society of India, 92: 145–156.

Kazmi, A.H., and Abbasi, I.A., 2008. Stratigraphy and historical geology of Pakistan. National Centre of Excellence in Geology, University of Peshawar, Peshawar, Pakistan, 1–524.

Kazmi, A.H., and Rana, R.A., 1982. Tectonic map of Pakistan, scale 1: 2000000 (1st edition). Geological Survey of Pakistan, Quetta.

Khalifa, M., 2005. Lithofacies, diagenesis and cyclicity of the lower member of the Khuff formation (late Permian), Al Qasim Province, Saudi Arabia. Journal of Asian Earth Sciences, 25: 719–734.

Khalifa, M., Kumon, F., and Yoshida, K., 2009. Calcareous duricrust, Al Qasim Province, Saudi Arabia: Occurrence and origin. Quaternary International, 209: 163–174.

Kummel, B., and Teichert, C., 1970. Stratigraphic boundary problems: Permian and Triassic of West Pakistan (1st edition). Department of Geology, University of Kansas, Special Publication, 4. Lawrence: University Press of Kansas.

López-Gamundí, O.R., 2010. Transgressions related to the demise of the Late Paleozoic Ice Age: Their sequence stratigraphic context. In: Lopez-Gamundi, O.R., and Buatois, L.A. (eds.), Late Paleozoic Glacial Events and Postglacial Transgressions in Gondwana, 468: 1–35.

Lu, Z., Zhang, S., Yin, C., Meng, H., Song, X., and Zhang, J., 2017. Features and genesis of Paleogene high-quality reservoirs in lacustrine mixed siliciclastic–carbonate sediments, central Bohai Sea, China. Petroleum Science, 14: 50–60.

Ma, P., Lin, C., Zhang, S., Dong, C., Zhao, Y., Dong, D., Shehzad, K., Awais, M., Guo, D., and Mu, X., 2018. Diagenetic history and reservoir quality of tight sandstones: A case study from Shiqianfeng sandstones in Upper Permian of Dongpu Depression, Bohai Bay Basin, eastern China. Marine and Petroleum Geology, 89: 280–299.

Mahboubi, A., Moussavi-Harami, R., Carpenter, S.J., Aghaei, A., and Collins, L.B., 2010. Petrographical and geochemical evidences for paragenetic sequence interpretation of diagenesis in mixed siliciclastic–carbonate sediments: Mozduran Formation (Upper Jurassic), south of Agh-Darband, NE Iran. Carbonates and evaporites, 25: 231–246.

Martin, J.R., Redfern, J., and Aitken, J.F., 2008. A regional overview of the late Paleozoic glaciation in Oman. Resolving the Late Paleozoic Ice Age in Time and Space. Geological Society of America, Boulder, Special Paper, 441: 175–186.

Melim, L., Westphal, H., Swart, P.K., Eberli, G.P., and Munnecke, A., 2002. Questioning carbonate diagenetic paradigms: Evidence from the Neogene of the Bahamas. Marine Geology, 185: 27–53.

Metcalfe, I., 2006. Palaeozoic and Mesozoic tectonic evolution and palaeogeography of East Asian crustal fragments: The Korean Peninsula in context. Gondwana Research, 9: 24–46.

Moore, S.E., Ferrel, R.E., Aharon, P., 1992. Diagenetic siderite and other ferroan carbonates in a modern subsiding marsh sequence. Journal of Sedimentary Petrology, 62: 357–366.

Morad, S., 1998. Carbonate cementation in sandstones: Distribution patterns and geochemical evolution. In: Morad, S. (ed.), Carbonate cementation in sandstones. The International Association of Sedimentologists Special Publication, 26: 1–26.

Moradpour, M., Zamani, Z., and Moalemi, S., 2008. Controls on reservoir quality in the lower Triassic Kangan formation, southern Persian Gulf. Journal of Petroleum Geology, 31(4): 367–385.

Nelson, R., 2001. Geologic analysis of naturally fractured reservoirs (2nd Edition). Gulf Professional publishing, an imprint of Elsevier, 1–232.

Roehl, P.O., and Choquette, P.W., 1985. Carbonate petroleum reservoirs (Edition 1). New York: Springer-Verlag.

Sanchez, C., and Galam, E., 1995. An approach to the genesis of palygorskite in a Neogene-Quaternary continental basin using principal factor analysis. Clay Minerals, 30: 225–238.

Schmid, S., 2004. Diagenesis and reservoir quality of the Sherwood Sandstone (Triassic), Corrib Field, Slyne Basin, west of Ireland. Marine and Petroleum Geology, 21: 299–315.

Schmoker, J.W., and Halley, R.B., 1982. Carbonate porosity versus depth: A predictable relation for south Florida. AAPG Bulletin, 66(12): 2561–2570.

Shah, S., 2009. Stratigraphy of Pakistan. Geological Survey of Pakistan Memoir 22, Quetta, Pakistan, 150–271.

Shehzad, K., 2019. Microfacies, diagenesis and reservoir characterization of Early Cretaceous Lumshiwal Formation in Nizampur area, Kala Chitta Ranges, Khyber Pakhtunkhwa, Pakistan (Unpublished M.s. thesis), Qingdao: China University of Petroleum, P.R. China.

Stephenson, M.H., and Al-Mashaikie, S.A.Z.A.K., 2010. New age for the lower part of the Kuhlan Formation, northwest Yemen. GeoArabia, 15: 161–170.

Stephenson, M.H., Jan, I.U., and Sa'ad Zeki, A., 2013. Palynology and correlation of Carboniferous–Permian glacigene rocks in Oman, Yemen and Pakistan. Gondwana Research, 24: 203–211.

Tahirkheli, R.K., 1979. The India-Eurasia suture zone in northern Pakistan: Synthesis and interpretation of recent data at plate scale. Geodynamics of Pakistan, 125–130.

Torsvik, T.H., Rousse, S., and Smethurst, M.A., 2010. Reply to comment by D. Aslanian and M. Moulin on ‘A new scheme for the opening of the South Atlantic Ocean and the dissection of an Aptian salt basin’. Geophysical Journal International, 183: 29–34.

Tucker, M.E., and Wright, V.P., 2009. Carbonate sedimentology. John Wiley and Sons, 1–496.

Vandeginste, V., and John, C.M., 2013. Diagenetic implications of stylolitization in pelagic carbonates, Canterbury Basin, offshore New Zealand. Journal of Sedimentary Research, 83: 226–240.

Vincent, B., Emmanuel, L., Houel, P., and Loreau, J.P., 2007. Geodynamic control on carbonate diagenesis: Petrographic and isotopic investigation of the Upper Jurassic formations of the Paris Basin (France). Sedimentary Geology, 197: 267–289.

Walter, L.M., 1983. New data on relative stability of carbonate minerals: Implications for diagenesis and cementation. AAPG Bulletin, 67: 566–566.

Welton, J.E., 2003. SEM petrology atlas. Chevron oil field research company, Methods in Exploration Series No. 4. Tulsa: American Association of Petroleum Geologists, Oklahoma, USA, 1–247.

Worden, R.H., Armitage, P.J., Butcher, A.R., Churchill, J.M., Csoma, A.E., Hollis, C., Lander, R.H., and Omma, J.E., 2018. Petroleum reservoir quality prediction: Overview and contrasting approaches from sandstone and carbonate communities. In: Armitage, P.J., Butcher, A.R., Churchill, J.M., Csoma, A.E., Hollis, C., Lander, R.H., Omma, J.E., and Worden, R.H. (eds.), Reservoir Quality of Clastic and Carbonate Rocks: Analysis, Modelling and Prediction. Geological Society of London, Special Publications, 435: 1–31.

Yeats, R.S., and Lawrence, R.D., 1982. Tectonics of the Himalayan thrust belt in northern Pakistan. US-Pakistan Workshop on Marine Sciences in Pakistan, Karachi, Pakistan, 39.

Yuan, Y., Cao, Y., Schulz, H., Hao, F., Gluyas, J., Liu, K., Yang, T., Wang, Y., Xi, K., and Li, F., 2019. A review of feldspar alteration and its geological significance in sedimentary basins: From shallow aquifers to deep hydrocarbon reservoirs. Earth-Science Reviews, 191: 114–140.

Zamanzadeh, S.M., Mirzaei, S., Abadi, M.S., and Poosti, M., 2011. Diagenetic factors controlling reservoir quality in the Faraghan Formation (Lower Permian), Darang Field, Southern Iran. Energy Exploration and Exploitation, 29(2): 109–128.

Zhang, J.L., Jia, Y., and Du, G.L., 2007. Diagenesis and its effect on reservoir quality of Silurian sandstones, Tabei area, Tarim Basin, China. Petroleum Science, 4(3): 1–13.

About the first author

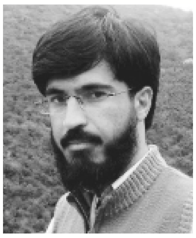

Muhammad ZAHIR, male, lives in Quetta, Balochistan, Pakistan. He has a B.Sc. from the University of Peshawar and M.Sc. from University of Balochistan. His study interest focuses on ichnofossils, sedimentology and sequence stratigraphy to understand the reservoir characteristics of the soft rocks. Previously worked with Pakistan Petroleum Limited and Oil and Gas Development Company Limited. E-mail: zahirkakargeo@gmail.com.

About the corresponding author

Mukhtiar GHANI, male, is currently serving at the Geological Survey of Pakistan. He received his B.Sc. and M.Sc. from University of Peshawar, and is currently working on his Ph.D. at the National Centre of Excellence in Geology, University of Peshawar. His research interest is reservoir sedimentology, sequence stratigraphy, structural geology, geochronology, and paleontology. E-mail: Mukhtiar.ghani@gmail.com.

Acta Geologica Sinica (English Edition) Calls for Submission of Review Papers

Acta Geologica Sinica (English Edition) is a bimonthly, SCI-indexed academic journal produced by the Geological Society of China. Having an impact factor ranging from 1.5 to 2.15, it has long been indexed by many international databases and websites, such as SCI, CA, BIG, etc. Internationally, the journal cooperates with John Wiley & Sons Co. Ltd to publish the electronic version; all papers can be downloaded online. Contributors wishing to submit, read, enquire and download can log in either via http://mc.manuscriptcentral.com/ags (English submission system).

In recent years, with the mining economy developing fast, geoscientists have been involved in all scientific activities from astronomy and the deep earth to oceanography and polar regions, from the macro to the micro world, and from the past to the future, leading to great achievements. In order to facilitate publication of these important scientific achievements, ***Acta Geologica Sinica*** (English Edition) intends to invite more open-dated submissions for review papers.

Manuscript Submission: during the preparation of manuscripts, authors are asked to follow carefully the guidelines presented.

Author or author grouping: a review paper, which is contributed by an author, an authoring group, or foreign coauthors, is given top priority, especially when offering an international vision, highly understanding of advances in international geosciences, and with a certain amount of SCI-indexed papers published.

Scope of articles: topics include stratigraphy, paleontology, tectonics, seismology, geophysics, lithology, geochemistry, ore deposits, sedimentation, oil and gas, hydrology, global climate change, etc., for example: progress and outlook in research on dinosaurs, ancient birds, insects, plants; global gold, iron or copper deposits, comprehensive utilization of coal gangue; eclogites.

Style of paper: manuscripts should include introduction, main body, development trend, conclusion and references. For geology, two types of paper are preferentially welcome: specific topics plus retrospective discussion and retrospective opinion plus current status.

No limitation to the number of pages: not less than 10 pages in general.

References: in order to follow the regulation of international geological counterparts, we suggest to authors to cite SCI-indexed papers, especially by international authors. Total number of references should be not less than 30.

Translation and polishing: for those who provide just Chinese-language version papers, the editorial office of *Acta Geologica Sinica* (English Edition) will help with translation and invite foreign expert/s to polish the manuscript so that it can meet publication requirements. Papers with fluent English and precise expression will be favorably published.

http://mc.manuscriptcentral.com/ags (English submission system)

Contacts:
FEI Hongcai, +86-010-68999024, feihongcai@163.com
FANG Xiang, +86-010-68990540, fangxiangcags@163.com